SOUTHERN PLAINS
TRANSPORTATION CENTER

ASSESSING THE RISK OF LANDSLIDE ON OKLAHOMA HIGHWAYS USING LIDAR

Yongwei Shan, Ph.D., P.E.
Srikanth Sagar Bangaru, M.S.
Joshua "Qiang" Li, Ph.D., P.E.
Xiaoming Yang, Ph.D., P.E.

SPTC15.1-35-F

Southern Plains Transportation Center
201 Stephenson Parkway, Suite 4200
The University of Oklahoma
Norman, Oklahoma 73019

DISCLAIMER

The contents of this report reflect the views of the authors, who are responsible for the facts and accuracy of the information presented herein. This document is disseminated under the sponsorship of the Department of Transportation University Transportation Centers Program, in the interest of information exchange. The U.S. Government assumes no liability for the contents or use thereof.

Technical Report Documentation Page

1. Report No. SPTC15.1-35-F	2. GOVERNMENT ACCESSION NO.	3. RECIPIENTS CATALOG NO.
4. TITLE AND SUBTITLE ASSESSING THE RISK OF LANDSLIDE ON OKLAHOMA HIGHWAYS USING LIDAR		5. REPORT DATE August 2017 6. PERFORMING ORGANIZATION CODE
7. AUTHOR(S) Yongwei Shan, Ph.D., P.E. (Principal Investigator) Srikanth Sagar Bangaru, M.S. (Graduate Research Assistant) Joshua "Qiang" Li, Ph.D., P.E. (Co-Principal Investigator) Xiaoming Yang, Ph.D., P.E. (Co-Principal Investigator)		8. PERFORMING ORGANIZATION REPORT
9. PERFORMING ORGANIZATION NAME AND ADDRESS Oklahoma State University School of Civil and Environmental Engineering 207 Engineering South, Stillwater, OK 74078		10. WORK UNIT NO. 11. CONTRACT OR GRANT NO. DTRT13-G-UTC36
12. SPONSORING AGENCY NAME AND ADDRESS Southern Plains Transportation Center 201 Stephenson Pkwy, Suite 4200 The University of Oklahoma Norman, OK 73019		13. TYPE OF REPORT AND PERIOD COVERED Final April 2016 – June 2017 14. SPONSORING AGENCY CODE

15. SUPPLEMENTARY NOTES
University Transportation Center

16. ABSTRACT

This primary objective of this study is to develop a comprehensive workflow to guide Oklahoma DOT to apply the LIDAR technology to landslide monitoring and risk assessment on Oklahoma highways. In addition to the primary objective, this study also aims 1) to evaluate registration and vegetation algorithms on the collected data, 2) to assess the displacement of the slope over various seasons, and 3) to assess the impact of vegetation removal and downsampling algorithms on slope displacement calculation. This study examined four different sites that include both rock type and soil type slopes on Oklahoma highways. Data were collected in four different seasons (summer, fall, winter, and spring) of the year. Then, a Multiscale Model-to-Model Cloud Comparison (M3C2) displacement analysis was performed on any of the two sets of data to identify the slope displacement. Throughout this study, technical challenges that were encountered are reported and the recommendations to overcome these challenges are reported as well. Through M3C2 analysis, it was observed that the largest change was observed between summer and fall. However, no significant change was observed in the majority of the areas of the slope, considering current level of registration error. It was found that vegetation removal and downsampling have impacts on the result of statistical displacement and significant change analyses. The comprehensive workflow developed in this study can guide ODOT step by step to implement the LIDAR technology to monitor and assess the risk of landslides on highways. The lessoned learned from this study can help ODOT have better plan for equipment acquisition, and data collection and analysis, if ODOT decides to adopt this technology.

17. KEY WORDS LiDAR, Landslide, Monitoring, Displacement Analysis		18. DISTRIBUTION STATEMENT No restrictions. This publication is available at www.sptc.org and from the NTIS.	
19. SECURITY CLASSIF. (OF THIS REPORT) Unclassified	20. SECURITY CLASSIF. (OF THIS PAGE) Unclassified	21. NO. OF PAGES 82 + cover	22. PRICE

SI* (MODERN METRIC) CONVERSION FACTORS

APPROXIMATE CONVERSIONS TO SI UNITS

SYMBOL	WHEN YOU KNOW	MULTIPLY BY	TO FIND	SYMBOL
		LENGTH		
in	inches	25.4	millimeters	mm
ft	feet	0.305	meters	m
yd	yards	0.914	meters	m
mi	miles	1.61	kilometers	km
		AREA		
in^2	square inches	645.2	square millimeters	mm^2
ft^2	square feet	0.093	square meters	m^2
yd^2	square yard	0.836	square meters	m^2
ac	acres	0.405	hectares	ha
mi^2	square miles	2.59	square kilometers	km^2
		VOLUME		
fl oz	fluid ounces	29.57	milliliters	mL
gal	gallons	3.785	liters	L
ft^3	cubic feet	0.028	cubic meters	m^3
yd^3	cubic yards	0.765	cubic meters	m^3
		NOTE: volumes greater than 1000 L shall be shown in m^3		
		MASS		
oz	ounces	28.35	grams	g
lb	pounds	0.454	kilograms	kg
T	short tons (2000 lb)	0.907	megagrams (or "metric ton")	Mg (or "t")
		TEMPERATURE (exact degrees)		
^oF	Fahrenheit	5 (F-32)/9 or (F-32)/1.8	Celsius	^oC
		ILLUMINATION		
fc	foot-candles	10.76	lux	lx
fl	foot-Lamberts	3.426	candela/m^2	cd/m^2
		FORCE and PRESSURE or STRESS		
lbf	poundforce	4.45	newtons	N
lbf/in^2	poundforce per square inch	6.89	kilopascals	kPa

APPROXIMATE CONVERSIONS FROM SI UNITS

SYMBOL	WHEN YOU KNOW	MULTIPLY BY	TO FIND	SYMBOL
		LENGTH		
mm	millimeters	0.039	inches	in
m	meters	3.28	feet	ft
m	meters	1.09	yards	yd
km	kilometers	0.621	miles	mi
		AREA		
mm^2	square millimeters	0.0016	square inches	in^2
m^2	square meters	10.764	square feet	ft^2
m^2	square meters	1.195	square yards	yd^2
ha	hectares	2.47	acres	ac
km^2	square kilometers	0.386	square miles	mi^2
		VOLUME		
mL	milliliters	0.034	fluid ounces	fl oz
L	liters	0.264	gallons	gal
m^3	cubic meters	35.314	cubic feet	ft^3
m^3	cubic meters	1.307	cubic yards	yd^3
		MASS		
g	grams	0.035	ounces	oz
kg	kilograms	2.202	pounds	lb
Mg (or "t")	megagrams (or "metric ton")	1.103	short tons (2000 lb)	T
		TEMPERATURE (exact degrees)		
^oC	Celsius	1.8C+32	Fahrenheit	^oF
		ILLUMINATION		
lx	lux	0.0929	foot-candles	fc
cd/m^2	candela/m^2	0.2919	foot-Lamberts	fl
		FORCE and PRESSURE or STRESS		
N	newtons	0.225	poundforce	lbf
kPa	kilopascals	0.145	poundforce per square inch	lbf/in^2

ASSESSING THE RISK OF LANDSLIDE ON OKLAHOMA HIGHWAYS USING LIDAR

Final Report

August 2017

Yongwei Shan, Ph.D., P.E., Principal Investigator
Srikanth Sagar Bangaru, M.S., Graduate Assistant
Joshua "Qiang" Li, Ph.D., P.E., Co-Principal Investigator
Xiaoming Yang, Ph.D., P.E., Co-Principal Investigator

Southern Plains Transportation Center
201 Stephenson Pkwy, Suite 4200
The University of Oklahoma
Norman, Oklahoma 73019

ACKNOWLEDGEMENTS

The authors would like to thank Southern Plains Transportation Center (SPTC) for providing the fund to support this study. The authors would like to thank Geotechnical Engineer, Chris Clark, for providing his expertise when selecting sites for the study. In addition, we would like to thank Joshua France, the Support Manager of Riegl USA for providing a free full license of RiScan Pro.

TABLE OF CONTENTS

LIST OF TABLES

LIST OF FIGURES

EXECUTIVE SUMMARY

Landslides on highways can endanger human lives and surrounding properties. The current approach of dealing with landslide by Oklahoma Department of Transportation (ODOT) is primarily reactive because there is no effective monitoring mechanism to assess the risk of landslide properly. When the damage is already done, expensive repair follows because the repair process is time-driven and the use of resources may not be the most cost-effective. Traffic lane closure during the repair increases travel time and road users costs. This gives an opportunity to look for alternative practices. Several studies have proved that the LIDAR technology can be used to detect the slope changes in mountains. But there is no readily available generalized framework to apply this technology to monitor or assess the risk of a landslide along highways.

This primary objective of this study is to develop a comprehensive workflow to guide ODOT to apply the LIDAR technology. The secondary objectives of this study are 1) to evaluate registration and vegetation algorithms on the collected data, 2) to assess the displacement of the slope over various seasons, and 3) to assess the impact of vegetation removal and downsampling algorithms on slope displacement calculation. This study examined four different sites that include both rock type and soil type slopes on Oklahoma highways. Data were collected in four different seasons (summer, fall, winter, and spring) of the year. Then, an M3C2 displacement analysis was performed on two sets of data collected at two different seasons to identify the slope displacement. Throughout this study, technical challenges that were encountered are reported and the recommendations to overcome these challenges are reported as well. Through M3C2 analysis, it was observed that the largest change was observed between summer and fall. However, no significant change was observed in the majority of the areas of the slope, considering the current level of registration error. It was found that vegetation removal and downsampling have impacts on the statistical result of the displacement and significant change analyses.

The comprehensive workflow developed in this study can guide ODOT step by step to implement the LiDAR technology to monitor and assess the risk of landslides on highways. The lessons learned from this study can help ODOT have a better plan for equipment acquisition, and data collection and analysis, if it decides to adopt this technology for landslide monitoring.

1. INTRODUCTION

1.1 Problem Statement

Landslides that occur on major highways endanger drivers and surrounding properties. Oklahoma Department of Transportation's (ODOT's) current practice in dealing with landslides is reactive. Cleaning and repairs are undertaken after the fact, which results in costly repair and a longer period of road closures causing an inconvenience for road users. Monitoring the fill/cut slopes change over the time along the roads that pass through the mountainous area can be an effective approach to assessing the risk of landslide properly and proactively deploy prevention, mitigation measures, or emergency response to reduce the impact of landslides. To address this issue, the use of terrestrial Light Detection and Ranging (LiDAR) technology was examined by a plethora of previous studies (Abdel-Razek) and it was found that terrestrial LiDAR is a technically feasible solution for landslide monitoring. However, there is no generalized workflow that can guide potential users to apply this technology for landslide monitoring on highways. In addition to the development of the generalized framework, this study also focuses on the documentation of the technical challenges encountered while applying this technology as well as the documentation of the recommendations to address these technical challenges.

1.2 Objectives

The overarching goal of this study is to develop a comprehensive workflow to apply terrestrial LiDAR technology to monitor landslides on highways by evaluating the existing workflow identified in the literature through a case study of four slopes on Oklahoma highways. This study has several secondary objectives, as follows:

- Evaluating the process of data collection, registration, downsampling, vegetation removal and displacement analysis to identify technical challenges in the existing workflow and provide recommendations to address these challenges;
- Assessing the impacts of various data processing procedures (vegetation removal, and downsampling, and registration error) on displacement analysis; and

- Quantifying the slope change over various seasons of the year

1.3 Organization of the Report

This report consists of five chapters:

- Chapter 1 describes the problem statement and objectives of this study.
- Chapter 2 includes a general introduction to landslides/rockslides and provides background information about the landslide monitoring techniques, principles of LiDAR technology, applications of terrestrial laser scanner, registration techniques, displacement analysis techniques, and comparisons of various displacement analysis techniques.
- Chapter 3 summarizes the monitoring site characteristics and data collection process. It also briefly explains all the data processing steps and tools required for this study. In the end, it describes the initially proposed research workflow for this study.
- Chapter 4 presents the result of registration, displacement analysis, and the comparison of slope displacement over various seasons. It also reports technical challenges and recommendations for registration process and displacement analysis. Moreover, it presents the generalized workflow of implementing terrestrial LiDAR.
- Chapter 5 summarizes all the findings of the research and the limitations of the research and future research in this area. In addition, practices regarding landslide mitigation are summarized from the literature.

2. REVIEW OF LITERATURE

2.1 Introduction to Landslides/Rockslides

Landslides are one of the natural catastrophes that result from the downward movement of the earth mass (Whittow 1984). They affect both the built environment and the natural environment directly or indirectly. They also cause human loss and substantial property damage (Fernandez Merodo et al. 2004). In mountainous areas, many road sections bear certain risks of landslide/rockslide or falling rock, causing blockage or damage to the roadway (Pfeiffer et al. 1993). According to United States Survey Fact Sheet 2004-3072, landslides cause loss of life and billions of dollars in property damage each year (USGS 2004).

S. Falemo & Andersson-Sköld (2011) developed a framework to quantify and visualize consequences of landslides using existing data and GIS-based weighted linear combination models. As a result, a map showing the geographical distribution of anticipated losses and landslide susceptibility was developed. Figure 1, shows relative landslide incidence and susceptibility across the United States.

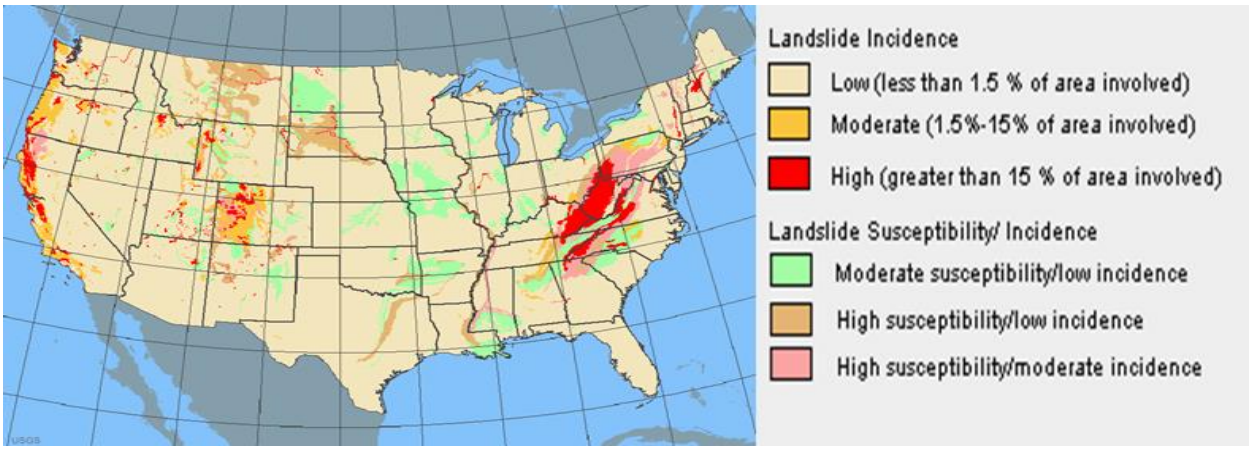

Figure 1. Landslide Incidence and Susceptibility Map (USGS Landslides)

Similarly, Amy B. Cerato et al. (2014) performed a real-time monitoring of slope stability in Oklahoma region; they proposed a landslide susceptibility map of Oklahoma by combining soil texture layer, slope derived from Digital Elevation Models (DEM), land cover from United State Geological Survey (USGS), etc. From this research, they concluded that southeast corner of

Oklahoma is highly susceptible to landslides. Figure 2 shows the landslide susceptibility of Oklahoma and the landslide events based on USGS and ODOT's data inventory.

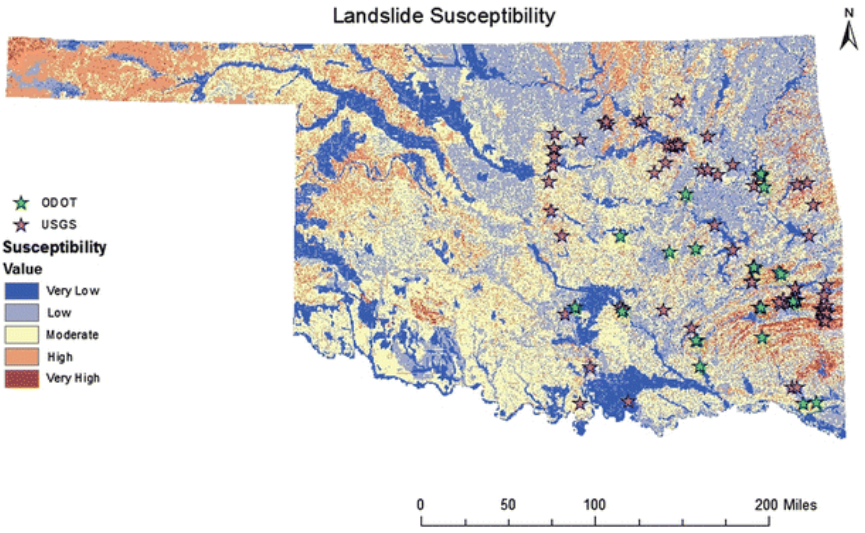

Figure 2. Landslide Susceptibility Map of Oklahoma

(Amy B. Cerato et al. 2014)

2.2 Mechanism and Influencing Factors of Landslides/Rockslides

Landslides occur when a slope changes from a stable condition to an unstable condition over time; these changes in slopes are caused by fluctuations in the effective stresses, changes in the material properties or variation of geometry (FEMA 2017). These changes are trigged by various factors like groundwater fluctuations, erosion, seismic activities, volcanic eruptions, heavy rainfall, freeze-thaw, and human activities, such as deforestation, blasting, earthworks, etc.(Wold and Jochim 1989). There are various types of landslides based on nature of the material involved and triggering mechanism. Rockslides are the fastest landslides (Varnes 1984), which are induced by rock failure where bedding plane of failure travels through intact rock from a cliff or other steep slope and causes the rock's instability, resulting in a massive blocks collapse (Bates and Jackson). As the blocks slide downslope, they can collide with other rocks and loosen other rocks on their way. Due to the gravity force, the broken pieces of rocks gain very high speed on the slope and travel a long distance, causing destructive damage to the properties and traveling traffic located on the path.

An increased incidence of extreme weather as a result of climate change can become a critical factor that triggers a landslide. Among extreme weather conditions, heavy rain is a common cause of landslide (FEMA 2017). For instance, because of excessive rains during June 2015, a rockslide occurred in Oklahoma's Arbuckle Mountains along the Interstate 35 (I-35) (Figure 3). Approximately 15,000 to 20,000 tons of fallen rock was removed, which caused a few weeks of lane closure at part of I-35 North, costing ODOT nearly one million dollars to repair (NewsOn6 2 2015).

Figure 3. Rockslide on I-35 near Davis, Oklahoma (Source: News Channel 4, KFORD.com)

Moreover, an earthquake is an emergent factor in Oklahoma that may contribute to landslides. As per the Oklahoma Geological Survey (OGS 2017) earthquake report, 2,325 earthquakes of magnitudes 3.0 or above were reported as of June 24th, 2016. Figure 4 shows the distribution of earthquakes over Oklahoma region. From the map, it can be concluded that central and southeast regions are more susceptible to earthquakes. Over the last five years, the number of felt earthquakes has quadrupled. Increased extreme weather conditions in Oklahoma, such as floods, tornados, and drastic temperature fluctuation, may induce more occurrences of landslides in the mountainous areas of Oklahoma.

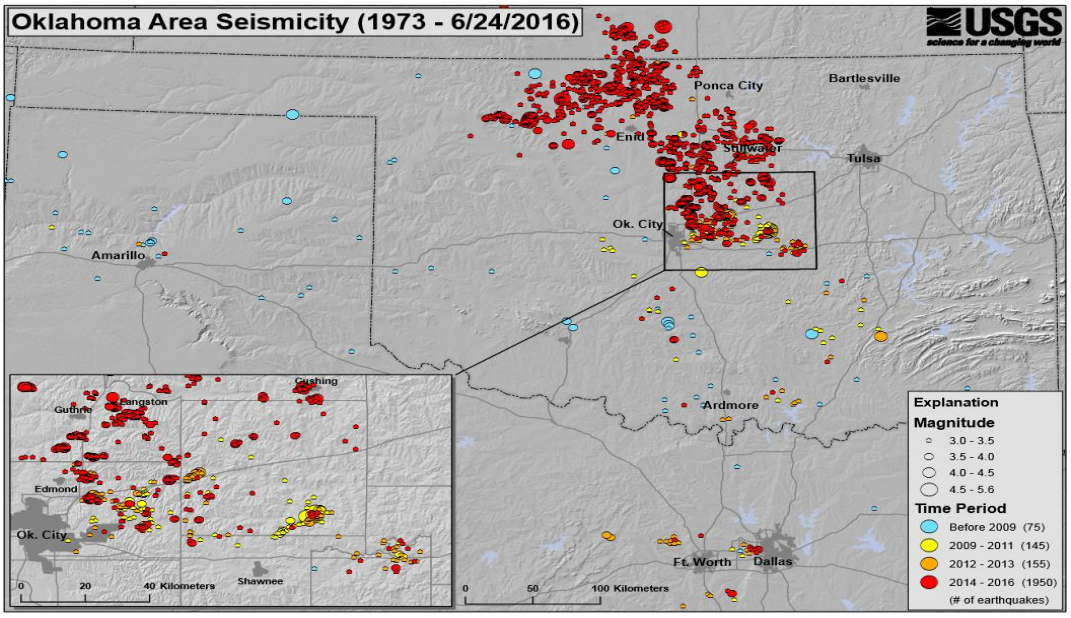

Figure 4. Seismicity Map of Earthquakes in the State of Oklahoma (USGS Earthquakes OK 2016)

2.3 Evaluation of Landslide Hazards

Landslide prediction is very challenging (Wieczorek and Snyder 2009). Detailed instrumental monitoring is valuable for the evaluation and prediction of landslides, but challenges exist including a lack of expertise or insufficient funds to purchase instrumentation and subsurface exploration. The major challenge in the instrumental monitoring is the selection of a particular small area for intensive investigation. For the selection of potentially hazardous areas, information regarding historical landslide events and current observations have to be studied. The slope movements in a region can be assessed by incorporating indicators like seismic activity, rainfall intensity, groundwater level, etc., but some of the landslides cannot be predictable by triggering event because they are occurred due to subsurface failures (Wieczorek and Snyder 2009).

2.3.1 United State Geological Survey's Landslide Monitoring Systems

Monitoring fill/cut slopes is an essential step to model the landslide behavior as well as to predict landslide occurrence (USGS 2017). Triggering mechanics and physics of landslides are a complex problem; research in these areas is still ongoing. Learning about landslides is a data-driven process. Therefore, scientists at the United State Geological Survey (USGS) Landslide Hazards Program

installed monitoring stations in ten selected sites that have frequent landslides to acquire more data to study the behavior of landslides. Various sensors and instruments are installed on site to monitor and measure the metrics that constitute good predictors of landslides, such as rainfall, groundwater pressure, soil water content, soil temperature, etc. Modeling and forecasting landslides is a continuous research effort for the USGS. In this effort, ten monitoring sites across the nation were selected and equipped with cameras, sensors, and gauging instruments to provide either real-time or periodic monitoring data (USGS 2017). Different sites may have different monitoring purposes. For example, while the monitoring site at Poplar Cove, Nantahala National Forest, North Carolina was established to support the research on hydrologic factors that influence landslide initialization; Colby Fire Monitoring Site in California was established to gain understanding of post-fire runoff, erosion, and debris-flow generation to help National Weather Service's decision makings in sending out warnings. Among those monitoring sites, slope movement or change over time is often collected because the process of slope change occurs slowly over a long period of time and slope change is a good indicator of the risks of potential landslides/rockslides.

2.3.2 Landslide Monitoring Techniques

Wieczorek and Snyder (2009) have proposed five basic steps for monitoring slope movement. These basic steps include (1) identification of types of landslides; (2) monitoring causes of landslides; (3) identification of materials involved in landslides; (4) determination of landslide displacement and (5) landslide regional risk assessment. Each one of these five vital signs includes three monitoring methods. Comparisons of these vital signs and monitoring methods based on technical needs, relative costs, and labor intensity are summarized in Table 1.

Table 1. Summary of Landslide Monitoring Vital Signs

(Wieczorek and Snyder 2009)

Vital Signs	Methods	Expertise	Technical needs	Relative costs*	Personnel	Labor intensity#
Types of landslides	1. Identification	Volunteer	No	A	Individual	Medium
	2. Measurement	Volunteer	Yes	B	Group	Medium
	3. Imagery	Scientist	Yes	C	Individual	High
Landslide triggers and Causes	1. Online Data	Volunteer	No	A	Individual	Medium
	2. Climatic and Seismic instruments	Volunteer	No	B	Individual	High
	3. Subsurface sampling and testing	Scientist	Yes	C	Group	High
Geologic materials in landslides	1. Examination	Volunteer	No	A	Individual	Medium
	2. Surface sampling	Scientist	Yes	B	Group	High
	3. Subsurface sampling and testing	Scientist	Yes	C	Group	High
Measurement of landslide movement	1. Tapes and GPS	Volunteer	Yes	A	Individual	High
	2. Extensometers	Scientist	Yes	B	Group	High
	3. Aerial photos, LiDAR and InSAR	Scientist	Yes	C	Group	High
Assessing landslide hazards and risks	1. Inventory	Scientist	No	A	Individual	High
	2. Volume, velocity and travel distance	Scientist	Yes	B	Individual	High
	3. Modeling	Scientist	Yes	C	Individual	High

Note: GPS—Global Positioning System; LiDAR—Light Detection and Ranging; InSAR—interferometric synthetic aperture radar* Relative Costs (in US$): A—up to $1,000; B—>$1,000–$10,000; C—>$10,000 #Labor intensity: low = <few hours; medium= <full day; high =>full day

Liu and Wang (2008) classified landslide monitoring techniques into three basic type: visual monitoring; instrumentation monitoring, and surveying. Visual monitoring techniques involve inspection using photographs and human inspection. Instrumentation techniques include installation of equipment such as piezometers and inclinometers for periodic or continuous data collection. A surveying technique involves physical measurement to detect surface movements. In the past, devices such as metal tapes or invar wire, levels, theodolites, Electromagnetic Distance Measurement (EDM), and total stations were used. In recent years, the use of aerial or terrestrial photogrammetry is widespread. In addition, other monitoring techniques include Global Positioning System (GPS), Interferometric Synthetic Aperture (InSAR), Light Detection and Ranging (LiDAR). These techniques also support monitoring landslide initiation and continuous movement. Table 2 summarizes typical range and precision for various monitoring techniques.

Table 2. Summary of Typical Range and Precision of Landslide Monitoring Techniques (Liu and Wang 2008)

Method/Technique	Results	Typical range	Typical precision
Precision tape	Distance change	<30 m	0.5 mm/30 m
Fixed wire extensometer	Distance change	<10-80 m	0.3 mm/30 m
Rod for crack opening	Distance change	<5 m	0.5 mm
Offsets from baseline	Coordinates differences (2D)	<100 m	0.5–3 mm
Triangulation	Coordinates differences (2D)	Variable <300 - 1000m	5–10 mm
Traverse/polygon	Coordinates differences (2D)	Variable, usually <100 m	5–10 mm
Leveling	Height change	Variable, usually <100 m	2–5 mm/km
Precise leveling	Height change	Variable, usually <50 m	0.2–1 mm/km
EDM (Electronic Distance Measurement)	Distance change	Variable, usually 1-14 km	1–5 mm + 1–5 ppm
Terrestrial photogrammetry	Coordinates differences (2D)	Ideally < 100 m	20 mm from 100 m
Aerial photogrammetry	Coordinates differences (2D)	H flight <500 m	10 cm
Clinometer	Angle change	±10degree	±0.01–0.1degree
Precision theodolite	Angle change	Variable	±10
GPS survey	Coordinates differences (2D)	Variable	2–5 mm + 1–2 ppm

Wang (2011) used permanently mounted GPS for monitoring landslide movements by analyzing changes in the GPS units. It is also proved that landslide movement can be measured within 2 mm, 6 mm in horizontal and vertical direction, respectively. But the main disadvantage of using this technique is the substantial costs involved in installing permanent GPS units. This technique is very suitable for monitoring landslides in highly populated areas.

Interferometric Synthetic Aperture Radar (InSAR) technique uses phase change between radar photographs to measure landslide movement. Rosen et al. (2000) explained how vegetation cover reduces correlation between radar photographs due to the volumetric scattering which affects the results of InSAR technique. Therefore, it is very difficult to apply InSAR in the densely forested environment.

2.4 LiDAR Background

Since last few decades, advancements in the field of electronics, photogrammetry, and computer vision have made it possible to develop consistent, high resolution, and accurate laser scanners or LiDAR. The laser scanners are non-contact 3D measurement instruments used to capture or record the geometry and sometimes textural information of visible surfaces of the objects or sites in a 3D digital representation – point cloud (Conner and Olsen 2014).

2.4.1 Measurement Principle of Laser Scanners or LIDAR

LiDAR works on the principle of measuring the time delay caused by the laser pulse traveling from source to the target surface and back to the instrument, which provides an easy way to evaluate the distance and angles (Vosselman and Maas 2010) (see Figure 5). Scanners are a line of sight technology: if the complete laser pulse reflects from an object, no points are detected behind the object, creating an occlusion (shadow). When only part of the laser pulse reflects back from a small object and the remaining light continues traveling, multiple X, Y, and Z coordinates (returns) can be obtained from one laser pulse (Renslow 2012). Multiple returns enable improved penetration of vegetation canopies compared to many other techniques.

The terrestrial laser scanners use the light transit time estimation measurement technique. In this technique, measurement of time delay is generated when the light travels from source to target and back to the source, which provides a method to evaluate the distance. Such systems are also known as time-of-flight measurement systems (Vosselman and Maas 2010). Light transit estimation measurement systems can also be realized by phase measurement technique, where laser systems emit a continuous wave to measure the time delay by determining the phase difference between transmitted and received signals.

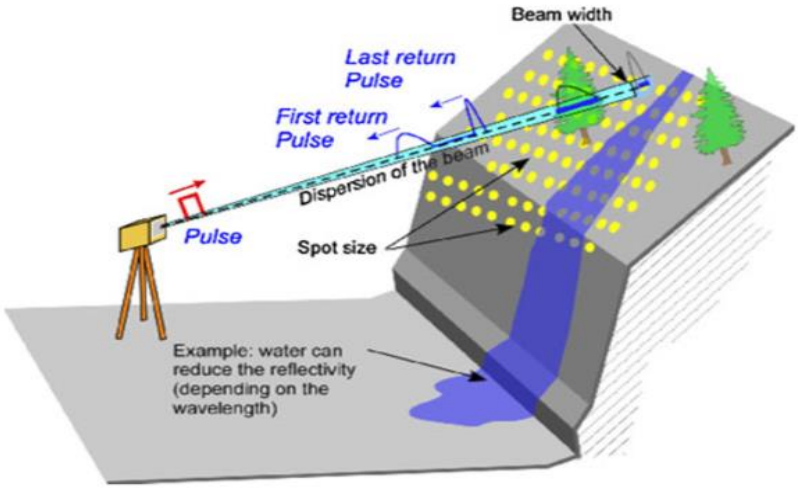

Figure 5. Principle of Laser scanner or LiDAR, Showing Example of Terrestrial Laser Scanner (TLS) (Jaboyedoff et al. 2010)

Based on measurement techniques, lasers are classified as pulsed lasers and continuous wave (CW) lasers. In both pulsed and CW laser systems, the position of the reflecting surface or object is relative to the scanner position which is known as a local coordinate system. Georeferencing transfers data from local coordinate system to global coordinate system (Conner 2013). By comparing the range resolution of pulsed and CW-lasers, it is observed that pulse laser system resolution is dependent on the resolution of time interval measurement. Whereas in CW lasers, the resolution depends on the frequency of the actual ranging signal. It is proved that, with an increase in frequency, higher range resolution can be achieved with CW systems. Wehr & Lohr (1999), through various system analysis and calculation, have proved that, if centimeter level of ranging accuracy is considered, pulse systems have higher accuracy than CW systems, in spite of high peak power. But to achieve sub-centimeter level accuracy, CW systems with high frequency have to be

used (Wehr and Lohr 1999). CW systems have very high data rates (up to 1Million 3D points per second for amplitude modulated CW systems) and limited operating range generally less than 100 meters. On the other hand, pulse based time-of-flight system is characterized by lower data rates but longer operational between 160 – 16000 meters (Vosselman and Maas 2010).

Time-of-flight systems measure more than one pulse echo due to multiple returns that are caused by object or site characteristics, particularly when vegetation is scanned. Wehr and Lohr (1999) also concluded that laser power is required when ranging are performed on non-cooperative targets. Therefore, the number of echoes measured depends on the type of scanner and target (Hofton et al. 2000). Usually, time-of-flight receivers can record four echoes per pulse. Time-of-flight scanners are often used in the following three main areas of topographic mapping: (I) Terrestrial laser scanning (TLS), (II) Airborne Laser Scanning (ALS), and (III) Mobile Laser Scanning (MLS).

2.4.2 Terrestrial Laser Scanning

Terrestrial laser scanners (TLS) are used in various applications, including agricultural and vegetation analysis, catastrophic mapping and analysis, terrain modeling, and industrial and structural modeling (Vosselman and Maas 2010). Compared to Airborne Laser Scanning (ALS) and Mobile Laser Scanning (MLS) systems, TLS systems have higher accuracy and precision. This is mainly because TLS systems are mostly used for smaller area data collection, typically less than a few miles (Conner 2013) and absence of real-time inertial and position measurements. Airborne laser scanner requires only one scanning direction, whereas another direction is provided by moving aircraft. In the case of terrestrial laser scanners, they are equipped with a 2D scanning device, which can rotate 360 degrees.

As discussed above in the LiDAR section regarding the range measurement principles, it was concluded that pulsed laser measurement systems provide high range capacity whereas phase measurement based continuous wave (CW) systems deliver high accuracy and data rate. Phase measurement based terrestrial laser scanners work with a range of 20 – 80 m and a range accuracy of 1 – 3 mm while pulsed laser based terrestrial laser scanners have a range of 250 – 1000 m with a maximum measurement accuracy of 5 -10 mm (Vosselman and Maas 2010).

TLS systems are usually operated on a tripod or bollard in a static position. Unlike ALS and MLS systems, TLS systems don't require vibration dampening system. Scanning is performed at a fixed position. Multiple scan positions are necessary to capture all components of an object or scene. The camera integrated with the terrestrial laser scanners are used to capture digital photographs of the scene, which can be registered to the point cloud data to add texture or color values to the point cloud. With the integrated bundle adjustment that involves fusion of data from all measurement devices such as a scanner, camera, and panoramic camera, a digital camera may also help in self-calibration of the laser scanner (Schneider and Maas 2007).

2.4.3 Applications of Terrestrial Laser Scanning

LiDAR has been widely used in a variety of areas in the field of civil infrastructure systems, including survey, site development design, urban planning, construction documentation, and asset condition assessment. For instance, Jaselskis et al. (2005) conducted a series of case studies and proved the effectiveness of using LiDAR in the area of soil and rock volume calculation and 3D as-built drawing creation. Kinzel et al.(2007) conducted an experiment on surveying a shallow, braided, sand-bedded river using LiDAR and compared the results with conventional survey methods; the research findings showed that the accuracy is comparable to conventional methods but that the productivity with LiDAR is an advantage over traditional surveying methods. Priestnall et al.(2000) demonstrated the possibility of using airborne LiDAR to create Digital Elevation Model (DEM) by removing the extracted surface features from a 3D surface model created by LiDAR. Chen et al.(2013) investigated the use of LiDAR for the evaluation of bridge damage due to vehicle collisions, surface erosions, and reinforcement corrosion. The information captured by LiDAR provides a specific measurement for damage analysis, which otherwise cannot be acquired by photogrammetry or plan photographic techniques. LiDAR can accomplish many tasks that would otherwise be difficult to perform with traditional survey instruments. It not only increases the productivity of surveyors by reducing the number of persons but also reduces the chance of exposing surveyors to safety hazards from traffic. Table 3 shows the different applications of LiDAR in landslide investigation.

Table 3. Applications of LiDAR in Landslides Investigation (Jaboyedoff et al. 2012)

Applications	Landslides	Rockfall	Debris flow
Detection and characterization of mass movements	Mapping of geomorphic features	Rock face imaging and characterization, calculating discontinuity orientation	Detection of mobilizable volumes, hydromorphone characterization
Hazard assessment and susceptibility mapping	Mainly as support for mapping	Some attempts for susceptibility and hazard mapping (not yet achieved)	Input for mapping hazard based on geomorphologic approach
Modeling	Classical modeling tools are not able yet to handle huge 3D information density; High-resolution DEM allow more accurate landslide modeling by improving geometrical characterization	High-resolution DEM for trajectory modeling	Input for spreading modeling
Mapping	Monitoring of surface displacement and volume budget	Monitoring of surface displacement, detection of pre-failure displacements, quantification of rockfall activity	Sediment budget, monitoring of morphologic changes in channels

2.5 Point Cloud Registration

Point cloud data registration is a crucial step in the entire data processing phase. Since terrestrial laser scanners are line-of-sight equipment, capturing the whole scene from a single scan position is often not adequate. It is required to record from multiple viewpoints to generate models of larger areas. Point cloud data from each scan position is in the scanner's local coordinate system. In order to combine different point clouds, it is necessary to transform different scans into a common coordinate system by estimating shifts and rotations between the scans. The process of determining the parameters of this transformation is known as registration.

During last few years, many methods have been proposed for registration of LiDAR data. Most of these techniques assume that data is homogenous, where data is compatible regarding point quality and density. These techniques result in inappropriate alignment parameters if the assumption is false, which is mainly due to improper weighting ratios of points. With advancements in laser scanning technologies, it is very important to addresses the registration of heterogeneous laser scans where the data is incompatible regarding point density and accuracy due to changes in the scanning mechanism and the mounting platform. The main reason for the motivation behind a registration process is to meet the need of aligning multiple scans from different scan positions into the common coordinate system to cover all the features of interest. For example, point cloud data acquired using tripod mounted LiDAR equipment are on scanner's coordinate system. Since scans from different positions are usually used to cover complex objects or larger areas, each of the required scans must be registered into the common coordinate system before further processing the data.

Various registration methods are available today, which vary in theory and implementation. The selection of registration techniques depends on the scanning mechanism and dataset. All these registration methods could be classified into three main categories: target-based registration, feature-based registration, and iterative closest point (ICP) based registration techniques. These techniques are discussed in the following subsections.

2.5.1 Target Based Registration

Static TLS can be used to monitor landslide displacements by installing targets on a landslide mass. Because of the robustness and accuracy, target based registration is more reliable compared to other registration methods. Typically, targets are highly reflective machined geometric entities (such as a disc, plate or sphere) mounted on a stable platform. For terrestrial scanners, these are usually 10 cm in radius. Becerik-Gerber et al. (2011) have explained the advantages and disadvantages of various targets, and also provide a study on the achievable accuracy of different targets. Figure 6 shows some of the 3D laser scanner targets used in the target-based registration technique.

Figure 6. Commonly used targets for terrestrial laser scanning

Even though using targets is more reliable, it is very expensive. It also requires a lot of preparation on site to setup them properly. In addition, these targets have to be positioned strategically between scanner positions (Reshetyuk 2010). Depending on the site, it may not be possible to place the targets at desired locations. Moreover, processing of such data requires manual effort to identify the same target in each scan and may depend on feature detection algorithms to detect these targets. In the case of heterogeneous data where data is collected at various times, using targets is not feasible. This is because it is not possible to maintain targets on site for a long period of time. In this case, it fails to setup common targets to perform heterogeneous point cloud data registration.

2.5.2 Feature-Based Registration

For the feature-based registration, a higher level of primitives is established to remove the cost and extra labor associated with setting up the signalized targets properly and to recognize the distinct points. Strategies that depend on a pre-preprocessing step to concentrate components of interest for the request to create conjugate elements for the registration fall normally under the class of

feature-based registration. Planar patches (Huang et al. 2012) created through a segmentation method can be used in the registration of overlapping scans. Rabbani et al. (2007) utilized planar components alongside barrel, circle, and torus that are the basic elements in the industrial sites. They proposed two strategies, direct and indirect techniques utilizing those geometric components. Indirect technique is fused for surmised registration through the minimization of the aggregation of squares of contrasts in parameters of models. Direct technique proposes concurrent registration of different scans by limiting the sum of the square distance of the points from the relating model surface utilizing the outcomes from the primary method as estimated values. Dold and Brenner (2006) suggested a computerized registration procedure for terrestrial laser scanning data utilizing extracted planar patches as geometric primitives. To avoid the lack of planar patches with different orientations and to enhance the registration outcomes, image data gathered from a hybrid sensor was integrated as additional information. This demonstrates a probability to incorporate extra information for the laser scanning data registration. Canaz (2012) fused photogrammetric data to register terrestrial laser scanning information with the least overlapping area. This work gave a relative evaluation of terrestrial laser scanning information registration utilizing both linear and planar components. Linear features (Chang et al. 2008) are extremely helpful for the registration of laser scans in urban regions since they can be inferred with a high level of automation. These linear features can be gotten from the intersection of planar objects which produce a line. On the other hand, the linear feature could likewise be pulled out from building edges in spite of the fact that they are known to create degraded accuracies because of the discrete way of LiDAR at break-lines. Catenary lines, for example, power lines in urban areas have been investigated as a source of control for covering LiDAR information for mobile mapping frameworks (MMS) adjustment and registration of overlapping datasets (Chan et al. 2013). The great capability of utilizing objects features has been demonstrated in few studies. The feature primitive is derived using a large number of LiDAR points, which results in a high confidence in extracting the features in a scene. Linear features are very reliable. In any case, the utilization of linear and planar features should be restricted to scenes that contain such primitives. Nevertheless, extraction of such features can be affected by noises and occlusions in the data (Rodrigues et al. 2002). Moreover, segmentation issues, for example, over-segmentation, and under-segmentation - if not settled - may prompt mistakes in the extracted features, which then can be passed to the registration step, thus degrading

the overall registration quality. The initial estimation of the transformation parameters among the features is also challenging and remains a subject of recent research (Al-Durgham et al. 2013).

2.5.3 Iterative Closest Point Registration (ICP)

The ICP is the most popular technique in use. There are many ICP variants and all of them assume that there exists an initial approximation between scans. Examples of the variants included in the studies presented by (Bae and Lichti 2008; Besl and McKay 1992; Rusinkiewicz and Levoy 2001). The algorithm consists of mainly a point-to-point matching procedure. Due to the assumption of point-to-point correspondence that is usually not true, final transformation parameters can be biased.

A primitive alternator representation is that one of the point clouds is undisturbed, whereas another cloud is converted to a higher order (e.g. triangles, planes). Although the model can be complex and takes more time to execute, the expected surface registration accuracy is higher (Beinat et al. 2006; Beinat et al. 2007; Boström et al. 2008; Habib et al. 2011). For instance, a variant of the ICP algorithm (Habib et al. 2010) uses triangular primitives in one input scan, and then the normal distance between points of the first scan and triangulated surface's second scan is then minimized.

In featured-based registration algorithm, the use of object primitives is even more complex, as illustrated in the work done by (Rabbani et al. 2007). The first step is the segmentation of point clouds to obtained useful objects (like cylinders). The next two steps are to fit the model and correspondence specification. To make sure that a good amount of geometric configuration information is obtained, a thorough check needs to be undertaken. Finally, the sum of squares of perpendicular distances along points and objects are minimized to get final registration. The obstacle one may find is that it is challenging to identify a feature in heterogeneous data due to the continuously changing level of difficulty and sampling of the overlapping scans. Since this registration method performs differently comparing to ICP and applies a different algorithm, it is called irregular of ICP.

In general, ICP-Variant is sub-grouped in three categories: Point-to-point, point-to-surface, and point-to-object. ICPatch and ICPP algorithms presented by Habib et al. (2010) belong to point-to-surface.

2.6 Displacement Measurement Techniques

One of the common data which is used to analyze landslide motion is LiDAR data. There is no such a method that analyzes the raw point data cloud and measures the 3D displacement field. A narrow list of methods was required based on qualitative metrics before performing any detailed performance tests. In order to identify the available methods, an in-depth literature review was performed. A preliminary evaluation was conducted to eliminate any poor performance techniques.

In order to find an appropriate technique for landslide displacement analysis, a survey of different techniques was conducted, and advantages and disadvantages of each technique are discussed below.

2.6.1 Point Cloud Based Displacement Measurement Techniques

Displacements can be measured using multi-temporal point cloud data. Landslide velocities and displacements can also be measured using these methods. Various available displacement measurement techniques are discussed in this section:

2.6.2 Point-to-Point Displacement Measurement Technique

This is a technique where each and every point measurement is made. The distance between two points (i.e. a point in compared cloud and a point in reference cloud) is measured. Point snapping and direct-measuring tools are used to measure in point cloud processing software manually. P2P is a common method used for rock mass characterization as well as rockfall analysis, but no landslide studies that utilized this technique in the literature were found. For obtaining geometric parameters of surface features and analyzing temporal changes in the object, P2P is an excellent technique, and it has many applications in fields, such as mechanical and structural engineering for measuring spot movements.

2.6.3 Cloud-to-Cloud Displacement Measurement Technique

P2P and cloud-to-cloud (C2C) are similar in principle, but C2C uses shortest-path distance. The distance between two points (i.e. a point in reference cloud and its nearest neighbor in the compared cloud), is measured (Figure 7A). Local model or height function can also be used to measure C2C distances – to represent the reference cloud's surface (Figure 7B). The local model is a best-fit planar surface centered at an arbitrary, pre-defined location in the reference cloud and interpolated using the points that fall within a pre-defined radius of that center point. Then the distance to the nearest point in the compared cloud is then computed in the direction normal to the local model.

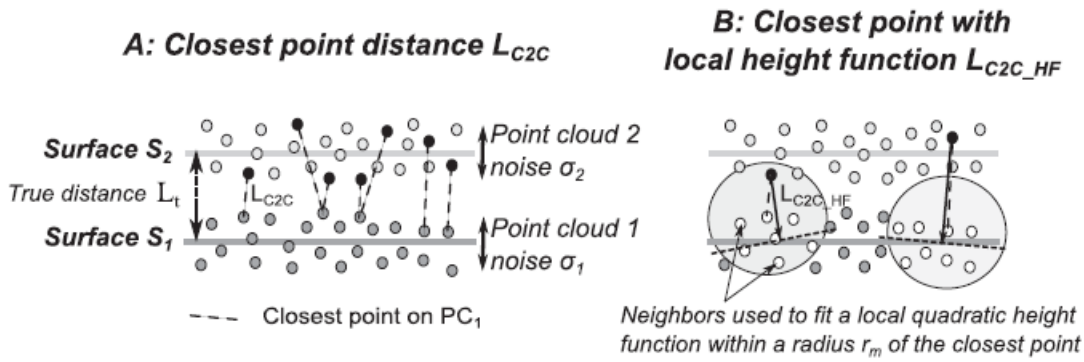

Figure 7. C2C Measurement Technique with Nearest Point (a) and Local Height Function (b) (Lague et al. 2013)

2.6.4 Cloud to Mesh (C2M) and Mesh to Mesh (M2M) Displacement Measurement Technique

C2M and M2M are similar measuring techniques that work on the same principles as that of the local version of C2C method except that they utilize globally fit surfaces instead of locally fit surfaces for their functioning. And for interpolating the surfaces, many methods are used such as kriging, inverse distance weighted averaging, Delaunay triangulation, etc., and each carries their own advantages and disadvantages. The key difference between the local and global interpolation is that, in the local interpolation, the point cloud data "fits" more closely but fails to capture the large-scale topography, whereas in the global models the data is "smooth" and designed to represent large-scale topography trends.

In C2M, the global surface is used to represent the reference cloud. It measures the distance to the nearest point in the compared cloud in the direction of the surface normal vector at given spacing

(Figure 8). M2M uses the global models for both clouds and measures the distance between the reference and compared surface at a certain given spatial interval and direction.

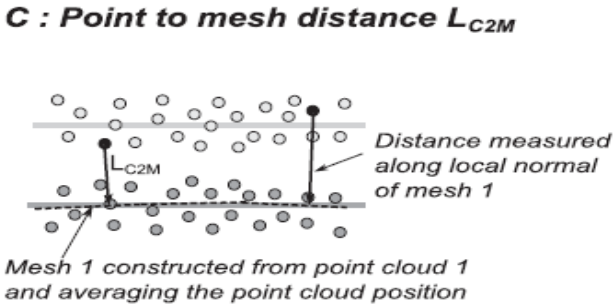

Figure 8. C2M Measurement Technique (Lague et al. 2013)

The M2M has two forms, the most widely used is known as DEM-of-Difference technique (DEMoD). This method interpolates the both reference and compared clouds elevation (z) values, such that raster data pattern is created called the Digital Elevation Model (DEM). The compared surface is then subtracted from the reference, and a new surface is generated with values that correspond to the difference in surface elevation. Generally, DEMoD is used in a landslide, slope stability, and rockfall analyses to calculate volumes of displaced materials and analyze slope movement (Baldo et al. 2009; Casson et al. 2005; Daehne and Corsini 2013; Dewitte et al. 2008). The second most common form of M2M is the slope normal method. This model can be of any form of surface model that represents the cloud geometry in a triangulated irregular network. The distance between the models is measured along the direction normal to the surface of the plane, usually with the positive direction of the Z-axis. This method hasn't been applied to landslides but is used in mechanical and structural engineering for getting area based displacement measurements.

2.6.5 Multiscale Model to Model Cloud Comparison (M3C2) Measurement Technique

The M3C2 model was developed to track displacements using time series laser scans in natural environments (Lague et al. 2013). This technique measures the distance between point clouds in a surface normal direction (Figure 9). The surface normal is calculated using a local model fitted to the points within a certain radius around each point in the reference point cloud. The radius can be set to a rough estimated value or can be set depending on the user-based experience. Another

smaller radius is drawn in the plane of the local model. It is the extended in the direction of the normal at a specified distance to form a cylindrical domain. All points from each cloud that fall within this domain are selected, and the average position of each set of points along the axis of the cylinder is identified. The average locations are considered as the position of the "surface" in each cloud, and the distance between them is the surface displacement measurement. The radii, cylinder length, and types of average used are user-defined.

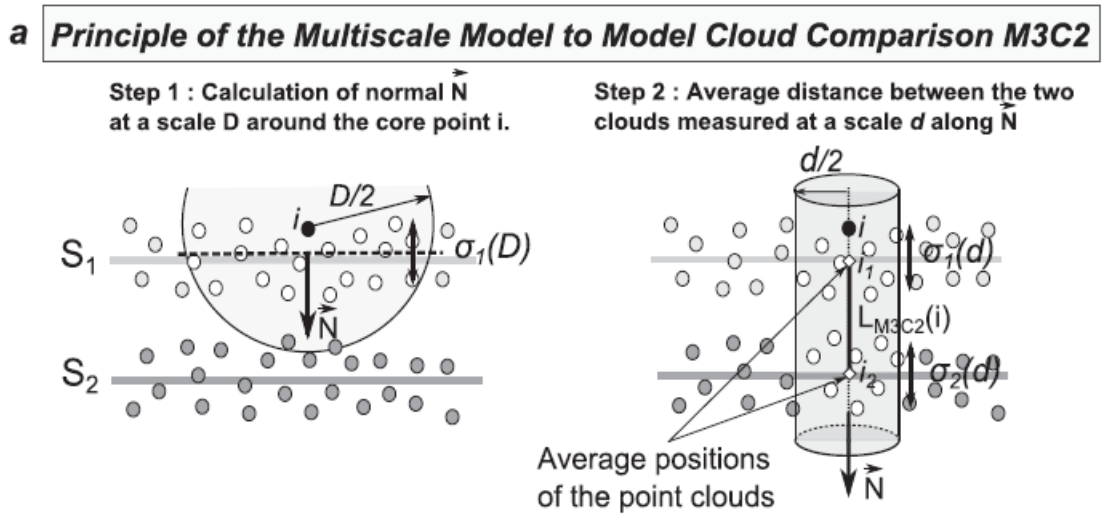

Figure 9. Principle of M3C2 Displacement Measurement Technique (Lague et al. 2013)

The methodology for M3C2 is summarized as follows (Figure 9):

- From initial point cloud, a set of points is chosen as subsample to perform the measurement. Subsampling is an optional step; it is performed only to reduce the calculation time.
- A surface normal vector is defined for each core point i by defining a plane which fits a set of points. The points NNi are within a sphere of radius D/2 of i. Where D is a normal scale. These vectors are oriented in the direction of user-defined orientation
- Roughness of the point cloud around i is calculated as standard deviation of distance between points on scale D
- The second step includes defining a cylinder with a radius d/2 where d is defined as projection scale. The axis of cylinder passes through the point i. The cylinder is extended both the direction of the axis to a maximum depth which manually defined. The cylinder intersects both the clouds and generated subset of points n_1 and n_2

- The mean distance between two point clouds is calculated along surface normal using n_1 and n_2 which are defined as i_1 and i_2. The M3C2 distance between two point clouds is the distance between i_1 and i_2.

The normal and projection scale have to be chosen based on the data roughness and point density. Higher the normal radius produces a smoother surface, which has less impact on the distance measurement.

The other attribute of M3C2 analysis is the Level of Detection (LOD), which takes surface roughness of both the point clouds and registration uncertainty into consideration. The M3C2 analysis also calculates the distance uncertainty based on Level of Change Detection ($LOD_{95\%}$). If the calculated $LOD_{95\%}$ is greater than the measured distance, then the change is considered as 'non-significant' and conversely, if the $LOD_{95\%}$ is less than the measured distance, then the measured value is considered significant at 95% confidence interval.

2.7 Advantages and Disadvantages of Various Displacement Measurement Techniques

A comprehensive literature review has been performed, and a summary of advantages and disadvantages of various displacement measurement techniques is presented in this section:

2.7.1 Advantages/Disadvantages of P2P

The primary advantage of P2P is that it helps the user to pick a precise measurement point and allow for the true point displacements. P2P doesn't depend on the surface modeling or interpolated point locations. The user can choose from individual data points and select the most appropriate points in each cloud (Haugen 2016).

The Disadvantage of P2P is that it is not accurate when small displacements are taken into account. The displacement measurements are not reliable and could be greater or smaller than the actual displacements when they are small (Haugen 2016).

2.7.2 Advantages/Disadvantages of C2C

The advantage of C2C is that it can generate measurements for the entire point cloud. It also successfully accounts for the local model for data variance. Thus the data spread on displacement measurements minimizes errors that are associated with global surface interpolation (Haugen 2016).

The primary disadvantage of C2C is that actual or true surface displacements cannot be measured by this technique. It measures the motion along the distance vector, and it can successfully measure true landslide displacement only if the landslide movement occurs in the direction normal to the surface, but in reality, landslides rarely exhibit such perpendicular phenomenon (Haugen 2016).

2.7.3 Advantages/Disadvantages of C2M and M2M

The primary advantage of C2M and M2M lies in the computational speed, usability, and the simplicity with which the raster and the global surface can be interpolated and measured with accurate displacements using a variety of software programs (Haugen 2016).

The primary disadvantages of C2M and M2M methods are errors arising from surface interpolation and spatial averaging. The spatial averaging occurs when point cloud data are smoothed due to global surface creation. The LiDAR point cloud data shows a spread of points around the actual surface, this surface may have some irregularities at a smaller scale than data spread. Moreover, surface interpolation is required for the point spacing of the data. Surface morphologies are clearly observed in zones at this scale. Point clouds with low or no density produce erroneous interpolation data as compared to the actual surface. Even the most advanced algorithms for interpolation fails to generate surface morphologies if the data obtained is below a certain specified threshold (Aguilar et al. 2010; Hodgson and Bresnahan 2004). Therefore, C2M and M2M measurements are not reliable if the point spacing is large (Haugen 2016).

2.7.4 Advantages/Disadvantages of M3C2

The primary advantage of the M3C2 technique is that it utilizes statistical methods to measure the position of the ground surface in the reference and compared clouds. It can also fit variation in

scale and magnitude of surface roughness of a local model to the data spread. Thus, validating both the variance in point cloud data and morphological surface changes in the generated data spread helps make computation process much simpler and easier for the optimal cylinder radius selection ((Haugen 2016).

The primary disadvantage of the M3C2 method is that it uses a surface-normal displacement process, which is computationally intensive and less reasonable. Surface-normal displacement motion in landslides may or may not be accurate measures of slope movement. The assumption that the majority of movement will occur in the direction normal to the slope may be valid in the case of vertical or near-vertical slopes but is not valid for shallower slopes since both horizontal and vertical movement may exist (Haugen 2016).

2.8. Summary

Although predicting landslides is a challenging task because the triggering mechanism of landslides is complex, various studies have proved that terrestrial laser scanning can be used to monitor the landslides and assess the risk of landslide/rockslides. However, there is not a readily available generalized workflow that guides practitioners to apply this technology to landslide monitoring. The literature says target based registration is more reliable registration technique, but it may not be true in all cases, which was observed in this study. This means there is a gap in addressing all the challenges in applying this technology, particularly the technical challenges encountered when applying this technology to different sites that have different geotechnical properties. None of the research focuses on providing the requirements in choosing the algorithm for data processing. From the various displacement measurement comparisons, it was observed that M3C2 technique has more advantages compared to other techniques. The only disadvantage of the M3C2 technique is that the results are influenced by surface roughness and normal scale. In order to overcome the influence of surface roughness, it was also explained in the literature that higher normal surface values would smoothen the surface and prevents the disorientation of Normals. To the research team's best knowledge, there is no generalized workflow to apply the LiDAR technology for landslide monitoring on highways and also none of the research reported the challenges of applying this technology.

3. METHODOLOGY

The application of 3D Laser Scanning/ LiDAR technology for landslide monitoring on highways involves mainly two steps:

- Data Collection
- Data Processing

This section explains each of these steps in detail.

3.1 Data Collection

Since slope change is of major interest in this study, LiDAR was used to perform data acquisition on the slope/s of selected locations. LiDAR scanning is a very efficient and non-intrusive surveying method that does not require traffic closure during the survey. However, safety measures have to be taken by using road work signs, road safety cones, and safety vests to avoid accidents due to moving traffic. Climate impacts play a significant role in the slope movement that may trigger a landslide or rockslide(FEMA 2017). In the state of Oklahoma, freeze-thaw, rain, and earthquakes are believed to be the factors that can significantly influence the slope change (OGS 2017). In order to understand the effect of weather scenarios on slope change, data collection is performed at each selected location during four different seasons of the year: 1) summer (June 2016), 2) fall (September 2016), 3) winter (December 2016), 4) spring (April 2017).

3.1.1 Site Description

For this study, four road sections with potential landslide risks were chosen by consulting a geotechnical engineer at Oklahoma Department of Transportation (ODOT). Two of these locations are on Interstate 35 (I-35) near Davis, Oklahoma and the other two locations are on US 82 near Lequire, Oklahoma. They were named as Locations 0 to 3. Figure 10 shows the geographical location of the four sites. Figures 11 and 12 are a close-up look at the sites. Figure 13 shows the pictures of four sites taken during data collection.

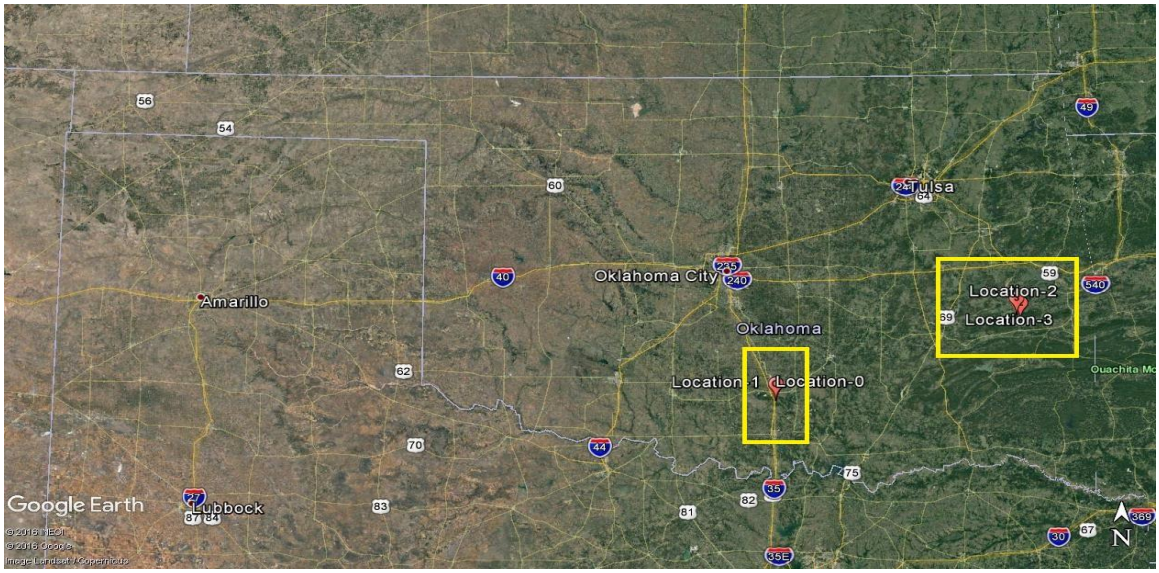

Figure 10. Location of Study Areas in Oklahoma area

Figure 11. Location 0 & Location 1 on I35

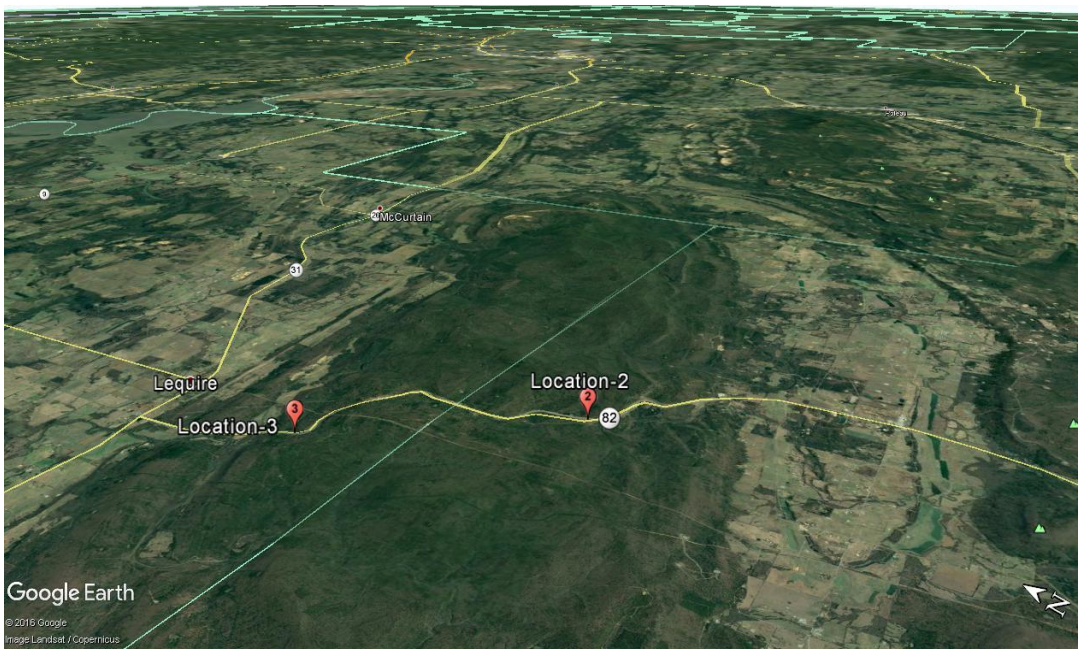

Figure 12. Location 2 & Location 3 on US 82

Figure 13. Pictures of the Slopes of All Four Locations

Table 4 describes the general description of the four locations

Table 4. Specifications of the Data Collection Sites

Location	Location on Highway	Slope Type	Length of Road Section (m)	Height of slope (m)
Location 0	I-35	Rock	209	25
Location 1	I-35	Rock	250	23
Location 2	US-82	Soil	240	22
Location 3	US-82	Soil	150	30

Four data collections were performed on each of the location, and each data collection was undertaken in one season (Table 5).

Table 5. The Corresponding Data Collection Dates for Each of the Locations

Location	June (Summer)	September (Fall)	December (Winter)	April (Spring)
Location 0	6/23/2016	9/27/2016	12/6/2016	4/5/2017
Location 1	6/23/2016	9/27/2016	12/6/2016	4/5/2017
Location 2	6/20/2016	9/30/2016	12/13/2016	4/7/2017
Location 3	6/20/2016	9/30/2016	12/13/2016	4/7/2017

3.1.2 Equipment Used

Compared to the traditional surveying, very few equipment is required for this application. A terrestrial LiDAR scanner was the primary equipment used during data acquisition, and it is not needed to be left at the site unattended for continuous monitoring. Following equipment (Figure 14) was used throughout the data collection process:

1. RIEGL VZ-400 Laser Scanner
2. Laptop with RiSCAN Pro software installed (Optional)
3. Tripod for scanner
4. Battery for the scanner

Figure 14. Equipment Used for Data Collection

Riegl VZ-400 terrestrial laser scanner was used for data acquisition (the instrument specifications are listed in Table 6). To record RGB values, a calibrated Nikon D700 digital single lens reflex (DSLR) camera was used. At the time of data acquisition, the scanner was always mounted on a tripod. A high capacity battery that supplies power to the scanner throughout the scanning process was used. Using laptop is optional, Riegl VZ-400 laser scanner supports stand-alone operation with an integrated Human-Machine interface. It supports internal storage up to 32GB and external storage via a USB 2.0 port. The main advantages of using a laptop with prescribed software package are a user-friendly interface, a 3D object view on the site, and an easy access to all settings. Except for Locations 2 and 3 during June, all the other data collection was performed using a laptop.

Table 6. Technical Specifications of RIEGL VZ-400 Laser Scanner (from www.riegl.com)

Parameter	Long Range Mode	High-Speed Mode
Laser Pulse Repetition Rate	100 kHz	300kHz
Effective Measurement Rate	42,000 meas./second	125,000 meas./second
Max Measurement Range (natural targets, □≥90%, highly reflective)	600 m	300 m
Max Measurement Range (natural targets, □≥20%, less reflective)	280 m	160 m
Minimum Range	1.5 m	1.5 m
Accuracy	5 mm	5 mm
Precision	3 mm	3 mm
Angular Measurement Resolution	Better 0.0005° (1.8 acrsec)	Better 0.0005° (1.8 arcsec)
Beam Divergence	0.3 mrad	0.3 mrad

3.1.3 Field Scanning

During data collection for each location, multiple scans from different scan positions were performed to ensure that the scans cover the entire scene from different angles. Table 7 shows a total number of scan positions for each data collection. For every data collection trip for each location, a RiSCAN Pro project was created and saved in .rsp file format. This project file contains scans of all scan positions. Whereas in the case of the scanner alone, it creates a .rxp file for each scan position. These .rxp files were used to recreate a RiSCAN Pro project. In the case of using a laptop, it is not required to recreate a RiSCAN Pro project. This is another advantage of using a laptop to operate the scanner. The scanner was operated in a high-speed mode with standard panorama settings (i.e., resolution = 0.08 degree). Each scan on an average collected 3 million points per scan position resulting in approximately 30 million points for each location per trip.

3.2 Data Processing

Data collected from all the four sites using the Riegl scanner were processed to obtain the landslide displacement. Data processing involves data registration, data down sampling, data filtering, and displacement analysis. The following subsections explain these processes:

3.2.1 Registration

The first and important step of data processing involves registration and merging of scans acquired at multiple scan positions for each location. All the registration algorithms used in this research are considered pairwise registration scenario. Due to the disturbance in some of the scans resulting from the obstruction of the digital camera by the antenna as well as the obstruction of the scanner by human or traffic, those individual scans were not used for the registration. In addition, scans without obvious planar features were also ignored. The importance of the planar features will be explained in the later sections. Table 7 shows the actual number of scan positions used for scanning and number of scan positions used for registration for all data collection.

Table 7. The Number of Scan Positions (SP) Used for Scanning and Registration by Location

Location	Collected SP (Jun.)	Regstr. SP (Jun.)	Collected SP (Sep.)	Regstr. SP (Sep.)	Collected SP (Dec.)	Regstr. SP (Dec.)	Collected SP (Apr.)	Regstr. SP (Apr.)
Location 0	5	4	9	9	12	12	10	9
Location 1	6	5	10	10	13	9	10	9
Location 2	4	4	6	3	12	5	10	3
Location 3	4	4	9	5	11	11	10	10

From Table 7, it is observed that Location 2 uses very few scan positions for registration due to the absence of planar features. Since the data was collected without using targets or GPS, feature-based registration and iterative closest point (ICP) technique were used to register this data.

In this project, all the scans of each data collection were primarily registered using the scanner manufacturer's data processing software, RiSCAN Pro with Multi-Station Adjustment (MSA) plugin. The data registered using this technique was used for further processing. The following subsections explain all the registration techniques used in this project.

3.2.1.1 Coarse Registration

Coarse registration is the first step of the registration process which involves manual alignment of scans as close as possible, which can be performed using coarse registration tool in RiSCAN Pro or CloudCompare (open source software used to process 3D point cloud or mesh data). This process involves picking a few pairs of corresponding points in each scan (Figure 15). Most of the points were picked from the sign boards available on the highway. Coarse registration is performed using RiSCAN Pro throughout this project (See Appendix for the process).

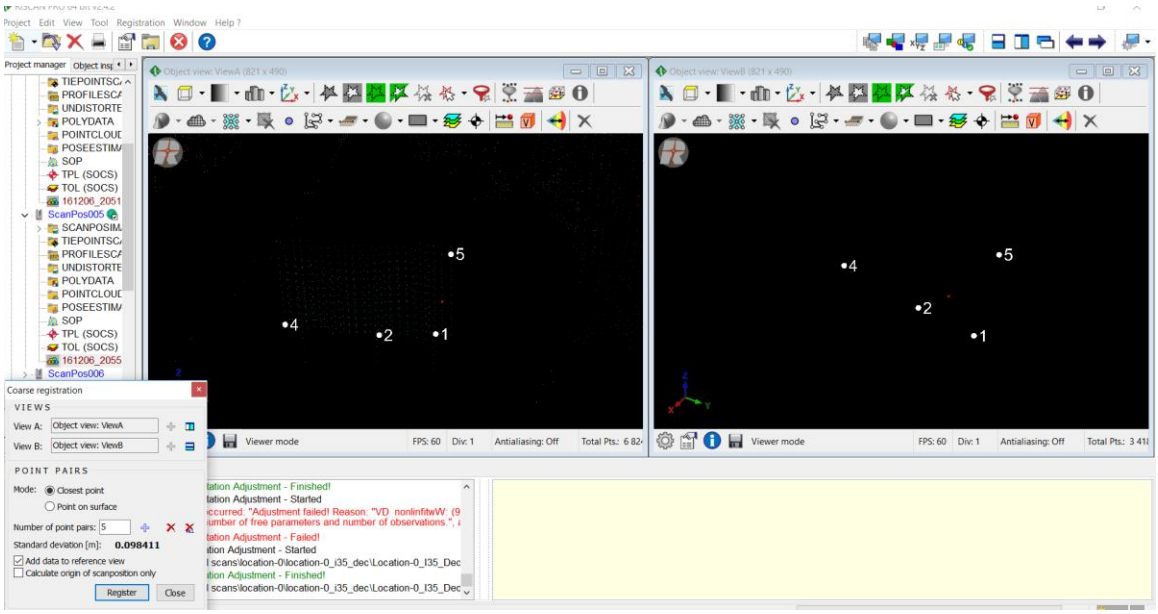

Figure 15. Coarse Registration Using RiSCAN Pro

3.2.1.2 Fine Registration

Fine registration is the process of refining the point clouds alignment obtained in the coarse registration. In this project, RiSCAN Pro Multi-Station Adjustment (MSA) algorithm was used for fine registration (See Appendix for the process). MSA algorithm uses polydata which is the filtered version of each scan to perform the plane patch registration process. A plane patch filter was used to create polydata. Various parameters have to be defined for plane patch filter. Parameters and their values are shown in Figure 16. A plane patch filter identifies and triangulates planar areas (plane patches) in each scan. The MSA algorithm then identifies a common planar patch from each scan and shifts the scan till the best match is obtained. These adjustments were performed for three iterations. The parameters required for MSA and values of parameters for three iterations are

shown in Table 8. All the scans aligned using MSA were exported into ASCII or .pcd format and merged into a single scan using CloudCompare for each data collection. This merged scan was used for further processing. In addition to MSA, other registration algorithms like ICP (using CloudCompare) and Normal Distribution Transformation (NDT) (using Point Cloud Libraries) were tested for this data. All these methods require a coarse registration.

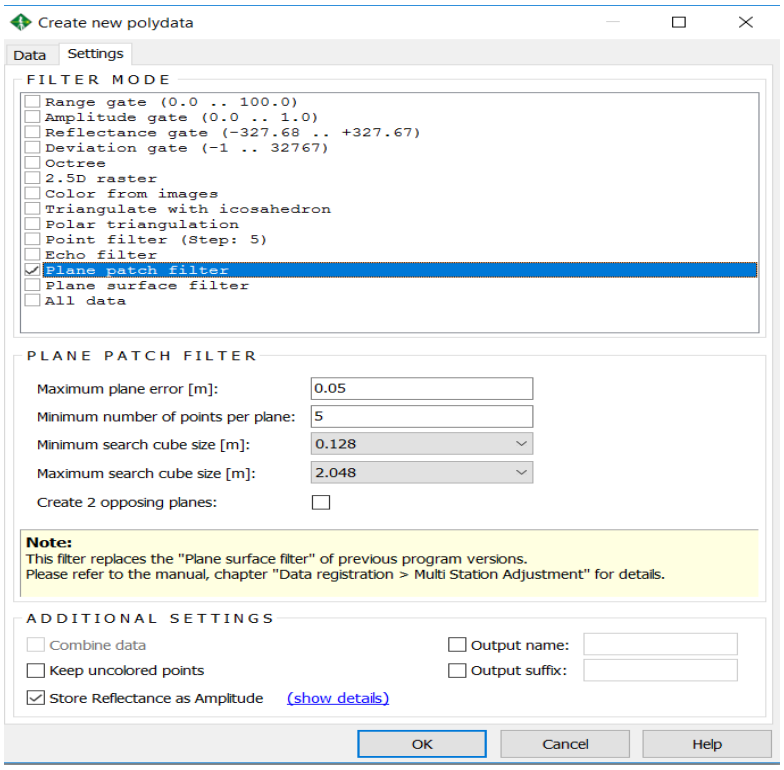

Figure 16. Parameter Values for Plane Patch Filter to Create Polydata in Multi-Station Adjustments (MSA)

Table 8. MSA Parameters and Their Values for Three Iterations

Parameter	First Iteration	Second Iteration	Third Iteration
Mode	all nearest points	all nearest points	all nearest points
Search radius(m)	0.5	0.2	0.1
Max tilt angle(deg)	5	5	5
Min. change of error 1 (m)	0.1	0.1	0.1
Min. change of error 2 (m)	0.05	0.005	0.005
Outlier threshold	2	2	2
Calculation mode	least square fitting	least square fitting	least square fitting
Update display	seldom	seldom	seldom

3.2.1.3 Merging and Aligning

For each data collection, scans registered using MSA were exported into ASCII or .pcd files. These scans were merged into single scan for each data collection using CloudCompare. For each data collection trip, a single merged scan was obtained, representing the data for a particular season. Merged scans of each season were aligned using CloudCompare and are used for further processing. Each of these registration processes has an error, which will be discussed in the later sections. The errors resulting from the registration and alignment processes were factored in the later displacement analysis.

3.2.1.4 Registration Error Analysis

Errors resulting from registrations can be carried throughout the data processing. As explained in the literature review section, systematic and random errors can be modeled mathematically and eliminated through system calibration procedures. But it is difficult to model the registration error (Brodu and Lague 2012). But in this project, errors obtained due to various registration steps were used to calculate a total error using the additive RMS error analysis which was proposed by Collins et al. (2009). The error calculated through this technique was used to identify the significance of the changes measured between two point clouds. The equation presented by Collins et al. (2009) is modified for this study as shown in Equation 1.

$$E_{total} = \sqrt{E_{reg}^2 + E_{alg}^2} \qquad \text{Eq. 1}$$

Where E_{total} indicates the total error that should be included in the displacement analysis, E_{reg} is the error associated with registration of scans using RiSCAN Pro, and E_{alg} is the error associated with alignment of two scans using CloudCompare. E_{reg} includes registration errors of all the scans obtained during MSA registration processes. For instance, for the displacement analysis of June and September's data, the E_{reg} includes the MSA registration errors of both June and September's data, which can be expressed as Equation 2:

$$E_{reg} = \sqrt{E_{June}^2 + E_{Sep}^2} \qquad \text{Eq. 2}$$

3.2.1.5 Segmentation

To focus on the area of the slope which is highly prone to landslide, this part of the entire location was segmented using interactive segmentation tool in CloudCompare. This was an edge-based segmentation. In order to segment similar patch from all seasons point cloud for a particular location, all these point clouds were aligned, and a patch was segmented using polygon edition mode by defining a 2D polygon on the selected point clouds. During this process, unwanted features and outliers were removed.

3.2.2 Downsampling

The size of the final merged scan of each data collection was very large. Large files slow down the data processing. In some cases, due to large file size, the CloudCompare shuts down. In this study, since we were working only on a particular area of the mountain which was usually lower in size, downsampling was not preferred. Therefore, downsampling of the point cloud was not a mandatory task. But to compare the displacements results of both original and downsampled point clouds with various algorithms, such as VoxelGrid filter (using Point Cloud Libraries) and subsampling (using CloudCompare), were used. The VoxelGrid filter (Libraries) creates a 3D voxel grid (basically 3D boxes in the space) over the input point cloud. In each voxel, all the points were approximated with respect to their centroid. Whereas in the case of subsampling using CloudCompare, point cloud was downsampled just by picking a random point and removing all the points around it. CloudCompare provides various methods, such as space (minimum distance

between points is specified), random (remaining points are specified), and octree (subdivision octree level is specified).

3.2.3 Vegetation Removal

Prior to the displacement analysis, vegetation removal was performed to reduce the noise due to vegetation. Similar to the downsampling, vegetation removal was an optional task depending on the characteristics of the site. Vegetation removal is required for Locations 2 and 3 since they have a thick vegetation which adds a lot of noise to the displacement measurement. Whereas for Locations 0 and 1, vegetation removal was not compulsory because both slopes are covered with rock and have less vegetation. Sometimes, vegetation removal may even remove part of rock portion of the mountain, which may provide inaccurate results. But to compare the displacement results of both vegetation removed and original point cloud, the multiscale dimensionality classification vegetation removal algorithm (Brodu and Lague 2012) was used. Multiscale dimensionality classification algorithm was applied to the point cloud using CloudCompare qCANUPO plugin developed by Lague et al. (2013).

3.2.4 Displacement Analysis

After analyzing the advantages and disadvantages of various displacement analysis algorithms, Multiscale Model-to-Model Cloud Comparison (M3C2) displacement analysis was chosen for this study. Since M3C2 algorithm measures the distance between two point clouds along the surface normal direction, this gives a proper understanding of the landslide. Lague et al. (2013) explains all the characteristics of the M3C2 algorithm and also its application to Rangitikei River data. In the current study, the M3C2 algorithm was applied using CloudCompare. The concept of M3C2 analysis is explained in the literature review section. In order to compare the displacement results, the analysis was performed on the vegetated surface (original patch), non-vegetated surfaces (vegetation removed patch), and downsampled (downsampled patch) point clouds. In order to obtain an accurate displacement, the analysis was performed only on a patch of the slope that is more prone to landslide. In order to perform M3C2 analysis, two point clouds are required, namely, reference cloud and data cloud. Displacement analysis measures the distance between the reference cloud to data cloud. In this project, four data collection trips were made between June 2016 and

April 2017. Pairwise displacement analysis between two different seasons' data was performed. The combinations for the displacement analysis are shown in Table 9.

Table 9. Various Combinations for Displacement Analysis

Seasons	Duration	Reference Cloud	Data Cloud
Summer-Fall	June-Sep	June	Sep
Fall-Winter	Sep-Dec	Sep	Dec
Winter-Spring	Dec-April	Dec	April
Summer-Spring	June-April	June	April

For detailed understanding of landslide displacement change, the displacement was calculated in X, Y and Z orientations. Normals diameter is one of the main parameters for M3C2 analysis (Figure 17); Normals for the reference cloud (Cloud#1) were calculated using "Normals Compute" in all three orientations. Based on a range of guess parameter (an option which predicts a range of values for the parameters based on the data) values, specific values were assigned to the parameters, such as projection scale and maximum depth. The values for Locations 1 and 3 are shown in Table 10; these values were kept the same for all seasons' comparisons. The core points are the subsample of reference cloud (cloud#1), where minimum distance between the points was chosen as 10 cm. The registration error calculated in the registration error analysis was included here. The direction of displacement measurement was along the Normals orientation. Apart from the displacement analysis, a significant change was also calculated. Significant change highlights areas in 3D where the measured change is significant. Usually, change is considered statistically significant if the level of change detection ($LOD_{95\%}$) is smaller than the measured change.

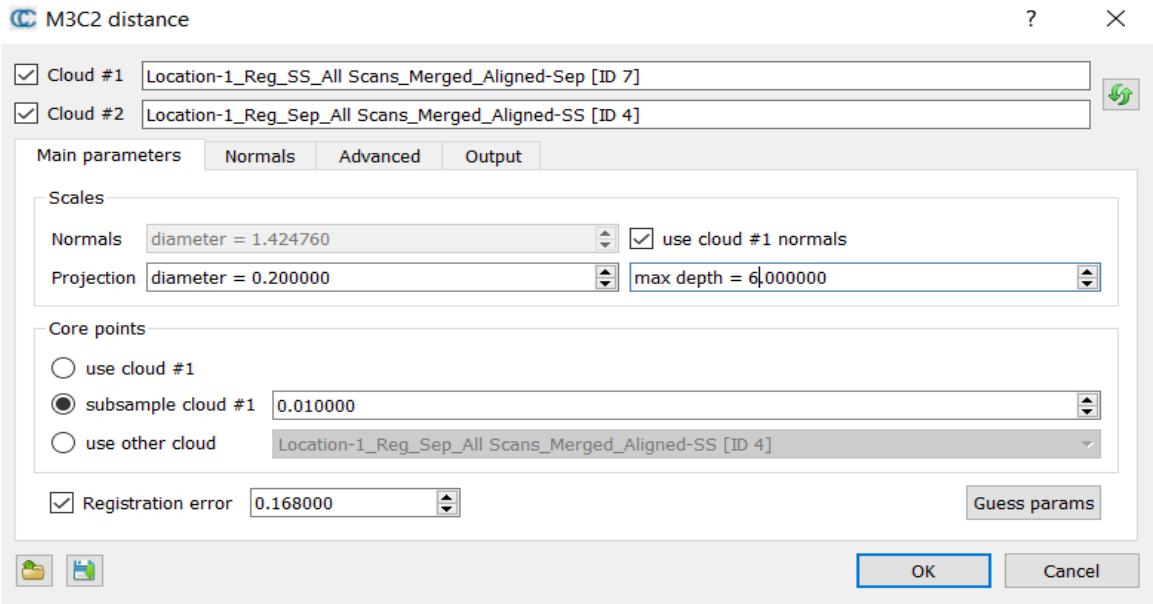

Figure 17. The Screen Shot of Main Parameters for M3C2 Distance Analysis

Table 10. M3C2 Displacement Analysis Parameter Values for Locations 1 and 3

Parameters	Location 1	Location 3
Normal Scale	0.5	13
Projection Scale	0.5	5
Max Depth	6	9
Subsample	0.01	0.01

3.3 Research Workflow

The Figure 18 below shows the initially proposed research.

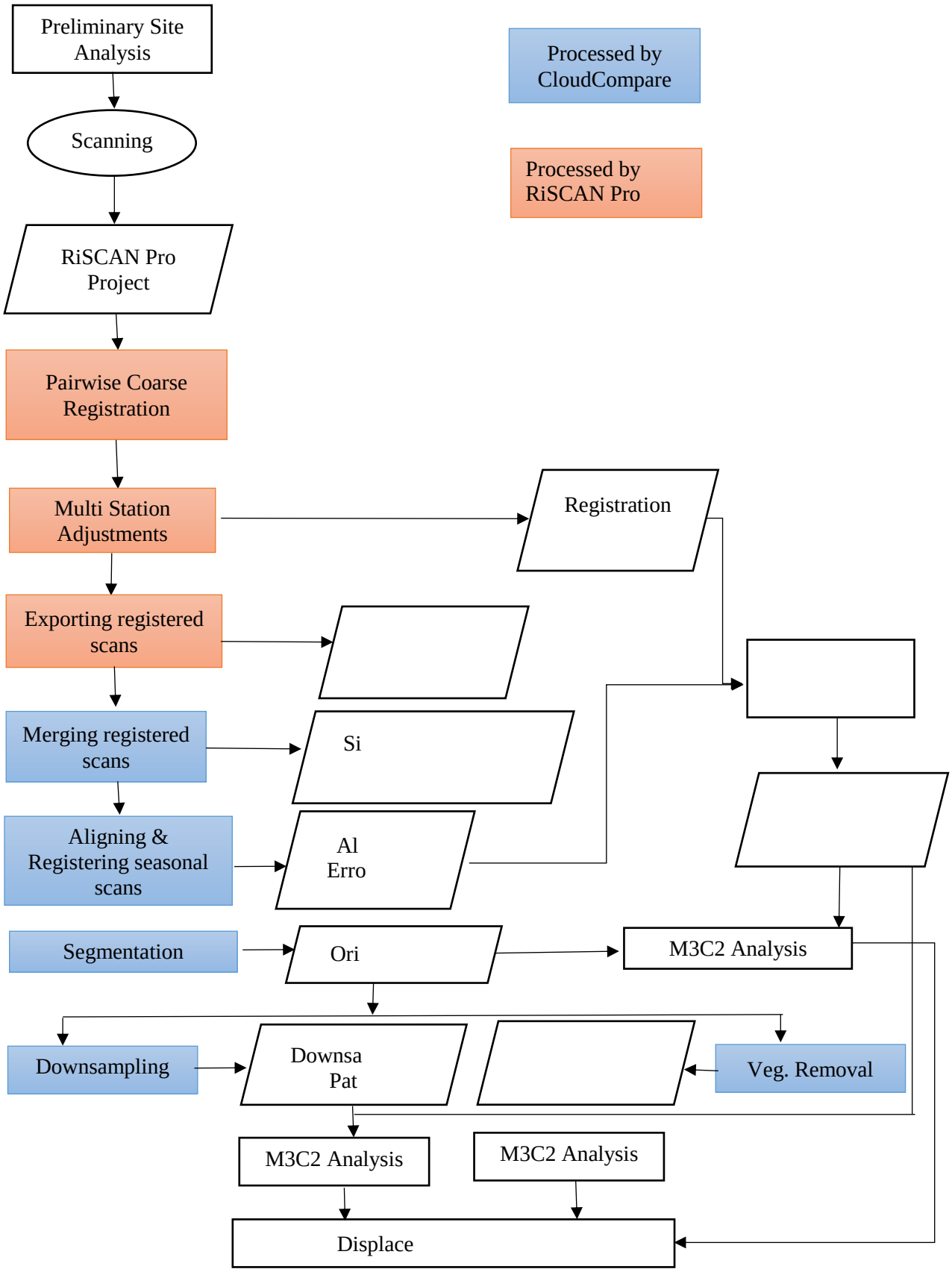

Figure 18. Initially P

4. RESULTS AND DISCUSSIONS

In order to achieve proposed objectives, various experiments on the process described in the previous section were performed. This section presents results of all experiments. As mentioned earlier, this study deals with four sites, namely Locations 0, 1, 2, and 3. Among these locations, Locations 0 and 1 are rock type slopes and Locations 2 and 3 are soil type slopes. For simplicity, results of one rock type slope (Location 1) and one soil type slope (Location 3) are presented in this section.

4.1 Registration Results

As mentioned in the methodology section, RiSCAN Pro software with Multi-Station Adjustment (MSA) plugin was used to register various scan positions for each data collection to obtain a single merged point cloud of a particular site. Along with RiSCAN Pro, other registration algorithms, such as Iterative Closest Point (ICP) and Normal Distribution Transformation (NDT), were evaluated on this data. A visual comparison was performed on the results of various registration algorithms.

4.1.1 Coarse Registration

Coarse registration is an essential step before applying multi-station adjustments using RiSCAN Pro. Coarse registration is the process of manual alignment of scans by picking corresponding points in two separate scans. Through various experiments, it was observed that accuracy of coarse registration depends on the closeness of the corresponding points chosen but not on the number of points. A weak correlation of 0.003 was observed between a number of points and standard deviation of coarse registration. The results of coarse registration are shown below. Figure 19 shows the orientation of two scan positions of Location 1 before and after the coarse registration. The number of points used for coarse registration and standard deviation error of coarse registration is shown in Table 11.

Figure 19. Scans Before (Left) and After (Right) Coarse Registration

From the above figures, it can be observed that coarse registration helps in aligning the scans more or less along the same orientation. Through various experiments and visual comparisons, it was concluded that the accuracy of fine registration depends on the quality of the initial alignment of two point clouds through coarse registration.

Table 11. Number of Point Pairs, Standard Deviation Error for Coarse and Fine Registration for Location 1

Item	Number of Point Pairs	Coarse Registration Error	Multi-Station Adjustments Error
Location 1-June			
Registration of SP 1-3	6	0.130	0.013
Registration of SP 3-4	8	0.090	0.014
Registration of SP 4-5	7	0.069	0.021
Registration of SP 5-6	8	0.069	0.018
Location 1-September			
Registration of SP 1-2	9	0.047	0.017
Registration of SP 2-3	11	0.073	0.018
Registration of SP 3-4	11	0.038	0.016
Registration of SP 4-5	11	0.046	0.015
Registration of SP 5-6	9	0.059	0.013
Registration of SP 6-7	8	0.043	0.015
Registration of SP 7-8	8	0.066	0.015
Registration of SP 8-9	9	0.109	0.016

Item	Number of Point Pairs	Coarse Registration Error	Multi-Station Adjustments Error
Registration of SP 9-10	8	0.057	0.017
Location 1-December			
Registration of SP 1-2	11	0.093	0.017
Registration of SP 2-3	11	0.084	0.015
Registration of SP 3-4	11	0.081	0.015
Registration of SP 4-5	13	0.129	0.015
Registration of SP 5-6	10	0.139	0.014
Registration of SP 6-7	10	0.081	0.014
Registration of SP 7-8	10	0.054	0.015
Registration of SP 8-9	10	0.126	0.015
Location 1-April			
Registration of SP 1-2	9	0.112	0.017
Registration of SP 2-3	11	0.051	0.014
Registration of SP 3-4	12	0.049	0.014
Registration of SP 4-5	10	0.050	0.012
Registration of SP 5-6	13	0.158	0.014
Registration of SP 6-7	13	0.135	0.016

4.1.2 Fine Registration

After the coarse registration was performed, multi-station adjustments (MSA) were applied to the scans. Multi-station adjustments refine scans' alignment and reduce the registration error. A similar procedure was followed for all the locations. For simplicity, only results of Location 1 are presented here. See Appendix for the results of other locations. Figure 20 shows the registration results of both before and after the fine registration for Location 1.

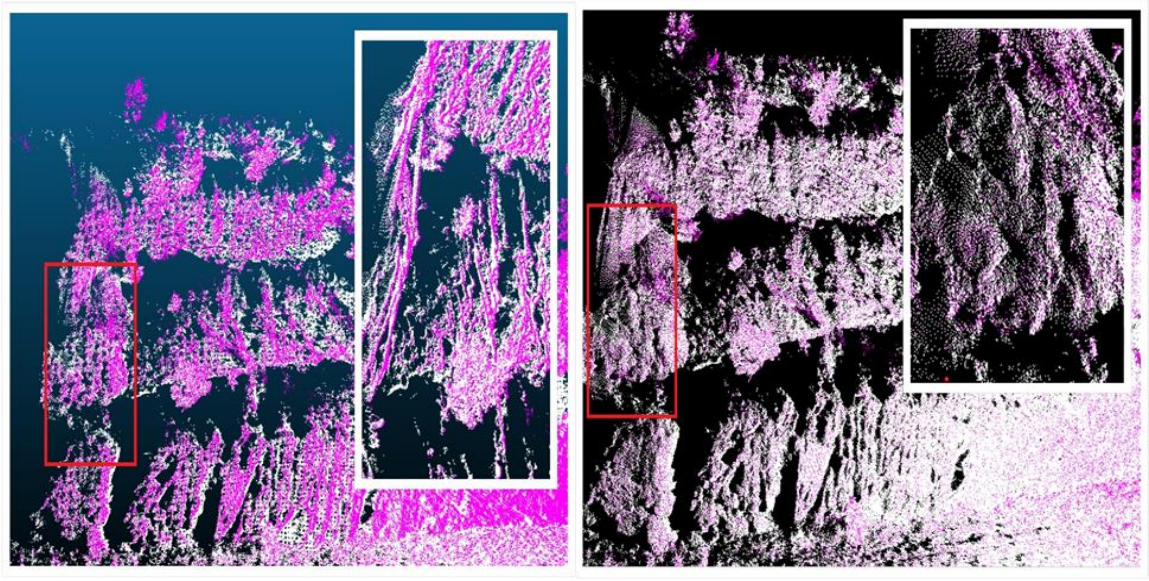

Figure 20. Before (Left) and After Fine (Right) Registration Using RiSCAN Pro for Location 1

From the result, it can be observed that, after the coarse registration, the scans were aligned approximately in the same orientation but were not completely overlapped. After applying multiple iterations of MSA, scans were finely aligned, and error was minimized (see Table 11). It was assumed that the MSA standard deviation error of fewer than 0.02 meters was desirable (Mapping 2013). Table 11 presents point pairs used for coarse registration and error in standard deviation for both coarse registration and MSA. It should be noted that the standard deviation error of MSA corresponds to the final iteration of the MSA registration.

4.1.3 Evaluation of Other Registration Algorithms

For each data collection, once all the scans were registered, they were exported and merged into a single dataset for each season. For every location, we have four single merged scans, which correspond to four different seasons (summer, fall, winter, and spring). In order to measure and compare the displacement over various seasons, displacement analysis was performed on two merged scans collected in two different seasons each time. In order to compute the displacement between two scans, two scans have to be aligned and registered. RiSCAN Pro does not support the importation and exportation of files from two different projects. In other words, it is not possible to merge two RiSCAN Pro projects, and neither does it support the importation of single merged scans into RiSCAN Pro software. Therefore, in order to register scans from different seasons, other

registration algorithms such as ICP (using CloudCompare) and Normal Distribution Transformation (NDT) (using Point Cloud Libraries) were evaluated. In order to compare the accuracy of the above-mentioned algorithms, registration was performed on coarsely registered scans of Location 1 collected in June using the files exported from RiSCAN Pro.

Figure 21 shows the result of the coarse registration and fine registration for Location 1 using ICP in CloudCompare. The RMS (Root Mean Squared) error obtained from ICP algorithm is much higher compared to the error from MSA. In the case of this example, the error obtained through ICP was 0.853 for 20 iterations and the error was 0.015 with MSA. It was also observed that with an increase in the number of iterations for ICP, RMS error was increased. Compared to the registration result of soil type slopes, ICP worked slightly better on rock type slopes.

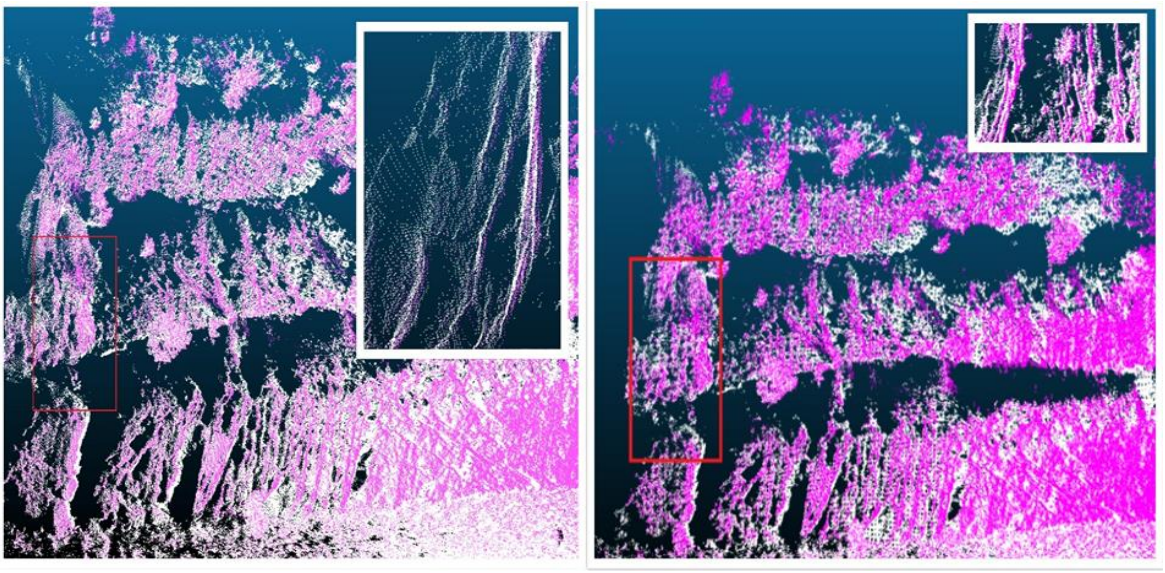

Figure 21. The Result of Coarse Registration (Left) and Fine Registration (Right) using ICP (CloudCompare) for Location 1

For Locations 2 and 3, the error was too high, and the scans were not aligned properly through visual check (Figure 22). This was mainly because of the absence of planar features and heavy vegetation.

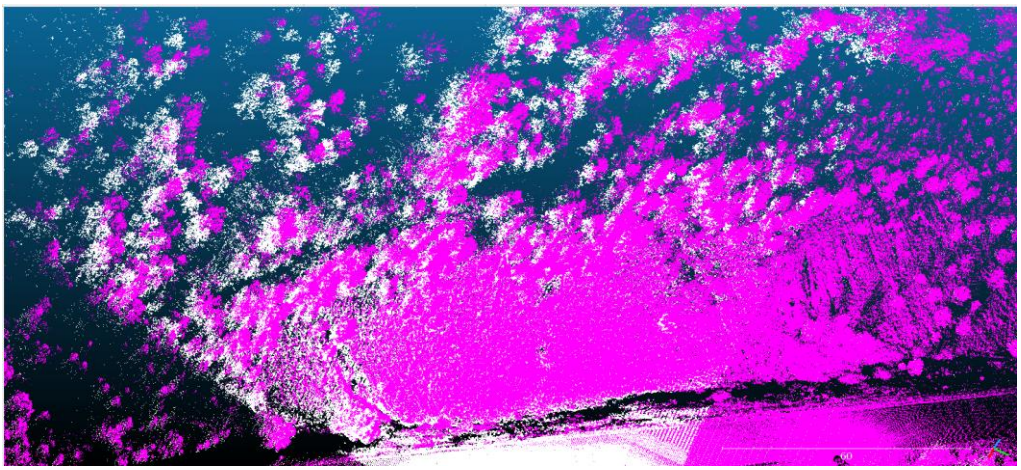

Figure 22. The Result of Fine Registration of Location 3 using ICP in CloudCompare

After applying the NDT algorithm on the coarsely registered scans, two scans were completely misaligned (Figure 23). Multiple trials were performed, but similar results were obtained. It can be concluded that NDT registration algorithm cannot be used on the data for this study.

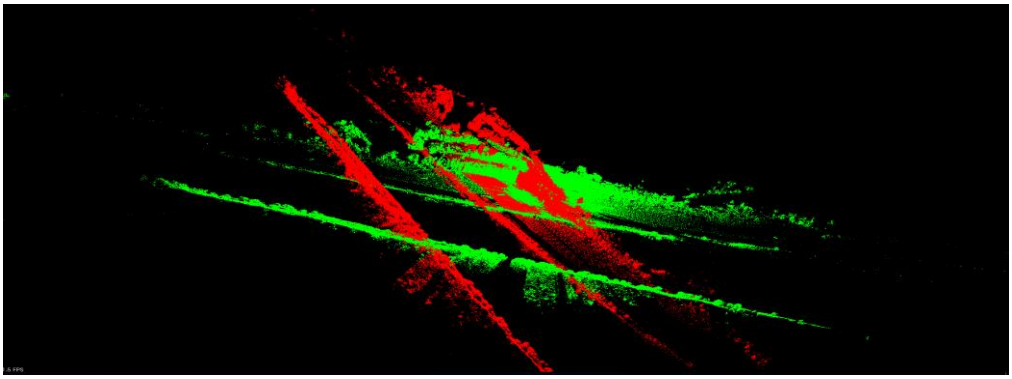

Figure 23. The Result of Registration of Location 1 with the NDT Algorithm

4.1.4 Results Registration Error Analysis

All the registration processes performed above involve errors, which are carried to the point cloud displacement analysis. Therefore, the M3C2 displacement analysis should take registration errors into account. As explained in the Section 3.2.1.5, Equations 1 and 2 were used to calculate the total registration error. The major registration errors include registration error due to RiSCAN Pro MSA (standard deviation of MSA iteration-3) and alignment error due to CloudCompare (RMS error during registration of two season scans). Table 12 shows the registration errors for Location 1. A similar analysis was performed for all the other locations.

Table 12. Registration, Alignment, and Total Errors for Location 1

Seasons	Registration Error
June	0.034
September	0.047
December	0.042
April	0.043

Seasons	Alignment Error
June-September	0.158
September-December	0.114
December-April	0.118
June-April	0.088

Seasons	Total Error
June-September	0.168
September-December	0.130
December-April	0.133
June-April	0.104

As mentioned earlier, alignment error is much higher compared to registration error. The total error obtained through this analysis was used later in the M3C2 analysis.

4.1.5 Technical Challenges and Recommendations for Point Cloud Registration

The major challenges experienced and lessons learned from the above results and site experiences during the registration process are as follows:

- Georeferencing was not used in this study due to the high cost of acquiring a high precision GPS unit for the scanner. As a result, various registration techniques were evaluated to choose the best algorithm that suits this data. Among all the registration techniques, feature-based registration (using plane patch filter in MSA) was effective. But this algorithm was not majorly successful in the case of locations with soil slopes; this was due to the presence of fewer planar surfaces and heavy vegetation. In order to prevent the above-mentioned situation, a preliminary site analysis is required before the start of

scanning. This analysis helps in identifying various features available on site and helps in choosing the registration algorithm to be used for future data processing.

- From the Table 7, it can be observed that, for Locations 2 and 3, fewer scan positions were used in registration. This was because the sign boards that were used for coarse registration were not properly scanned from those scan positions. The reason for this problem was that the sign boards are either not in the visible range of the scanner or occluded by traffic, the antenna of the equipment, or human. Nevertheless, this problem can be solved by choosing scan positions considering various factors such as distance, orientation from the reflectors/targets/planar surfaces. Avoid disturbances at the time of scanning and visually verify the scan at the end of scanning for each scan position.
- In some cases, it was observed that the registration was poor (scans were completely misaligned) despite very low error values. This was purely random. Therefore, a visual check as a "sanity check" is very important after every registration step.
- Due to the lack of full license for RiSCAN Pro, various tools had to be used for different processes. Using multiple tools may result in the following problems: losing the data, time-consuming processes, and file format incompatibilities. A decision on the selection of processing tools should be made in the preliminary site analysis stage based on the site characteristics and available resources.
- Even though there was no GPS unit, reflectors were used during the scanning process in order to use reflectors for coarse registration. But it was not unsuccessful; this is because the reflectors were not scanned completed or they were not clearly visible. This is due to incorrect selection of reflectors and choice of wrong reflector positions on site. A visual check for initial scans is required.
- The values for the parameters of plane patch filter and MSA are obtained through trial and error, which is a challenging task.

4.2 Results of M3C2 Analysis

One of the major objectives of this research is to analyze the change of slopes during various seasons. Registered scans obtained from the registration step were used for this analysis. In order to obtain more accurate results and a good understanding of the displacement, the analysis was

performed only on the portion of the slope which was more susceptible to landslide. The M3C2 analysis was also performed on vegetation removed data (vegetation removed patch) and downsampled data (downsampled patch) to understand the impact of vegetation removal and downsampling. The results of the M3C2 analysis are presented in this section. For simplicity, the M3C2 analysis results of Locations 1 and 3 are discussed in the later sections.

4.2.1 M3C2 Analysis on Original Patch

The data for analysis are in scanner's coordinate system. According to the scanner's coordinate system, Y- Axis represents the horizontal component, Z-Axis as a vertical component, and X-Axis as depth component. In order to obtain detail understanding of displacement change, the M3C2 analysis was performed on reference data along X, Y and Z Normals orientation. The analysis performed between scans each time, where one is considered as reference and other as a model. The distance was always measured from reference to the model. M3C2 analysis for Location 1 was performed using the values of the parameters mentioned in Table 10. The analysis results of Location 1 are shown below. The M3C2 analysis also includes significant change scalar field which represents the significance of displacement change. In the result of the significant change, the red color portion corresponds to a statistically significant change, and gray color corresponds to an insignificant change. The displacement was presented with a blue-to-red heat map. The negative values of M3C2 distance were shown in blue and positive values in red. In order to identify the slope movement at centimeter level, the scale of M3C2 distance was adjusted between 5 and 10 cm. In addition, Gaussian statistics were also calculated for each analysis.

4.2.1.1 M3C2 Analysis of June and September Scans

The analysis was performed on summer (June) and fall (September) seasons' data, where June scan was considered as reference and September scan was considered as a model. The significant change remains same along all orientations (Figure 24). The results of this analysis are presented along X, Y and Z orientations (Figures 25, 26, 27).

From Figure 24, it can be observed that only a small portion on the top right has a significant change. The change was approximately 0.55 meters. This is partly due to vegetation available in that portion. It was also observed that most of the displacement is insignificant, which is due to large registration error in the data in relation to the magnitude of displacement obtained. After

tweaking the parameter of registration error in the M3C2 analysis for multiple times, it was concluded that by lowering the registration error, more portions of the slope would show significant change.

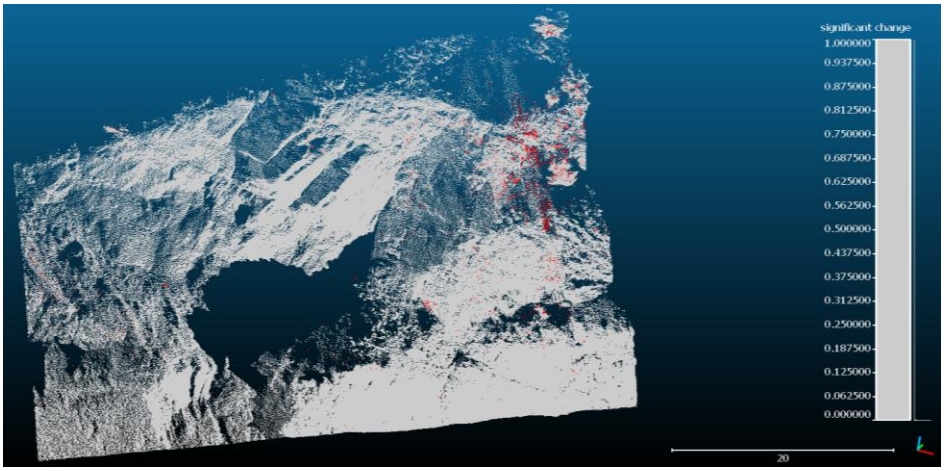

Figure 24. Significance of Change for June – September Scans

A mean change of 0.055 meters with a standard deviation of 0.03 was obtained along X-Axis (Figure 25). The positive value of displacement along X-Axis may be interpreted as a swelling in those portions.

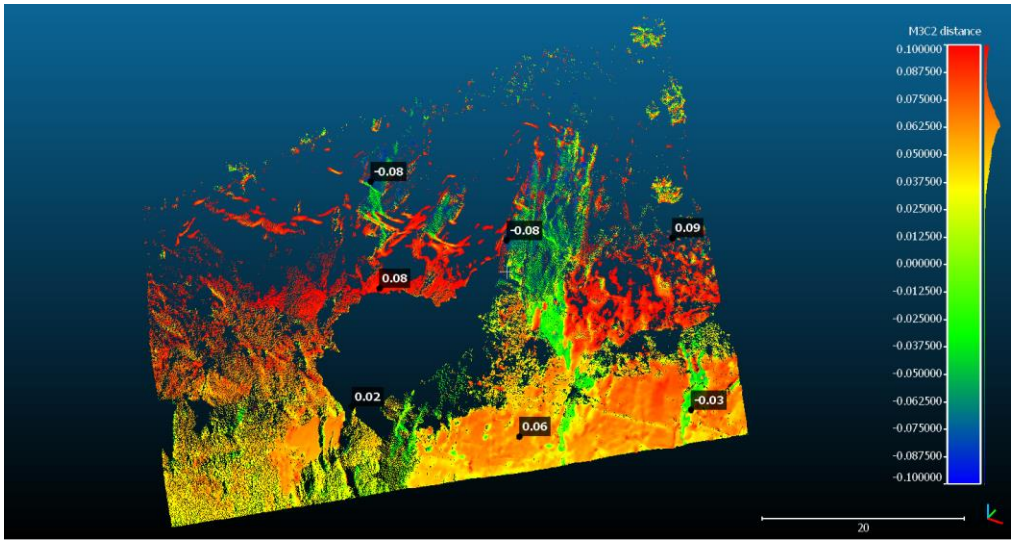

Figure 25. Displacement Heat Map of June - September Scans for Location 1 along X-Axis with Scale of 10cm

A mean change of -0.057 meters with 0.024 standard deviation along Y-Axis (Figure 26). The negative value of displacement along Y-Axis represents the movement in the horizontal direction.

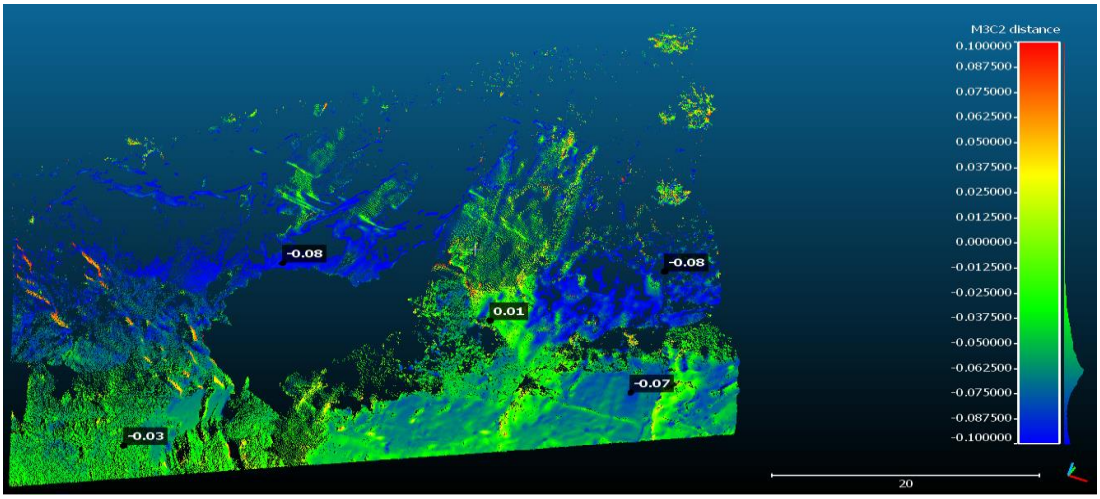

Figure 26. Displacement Heat Map of June - September Scans for Location 1 along Y-Axis with a Scale of 10cm

A mean change of 0.033 meters with 0.053 standard deviation along Z-Axis was observed (Figure 27). The positive value of displacement along Z-Axis represents the movement in the vertical direction.

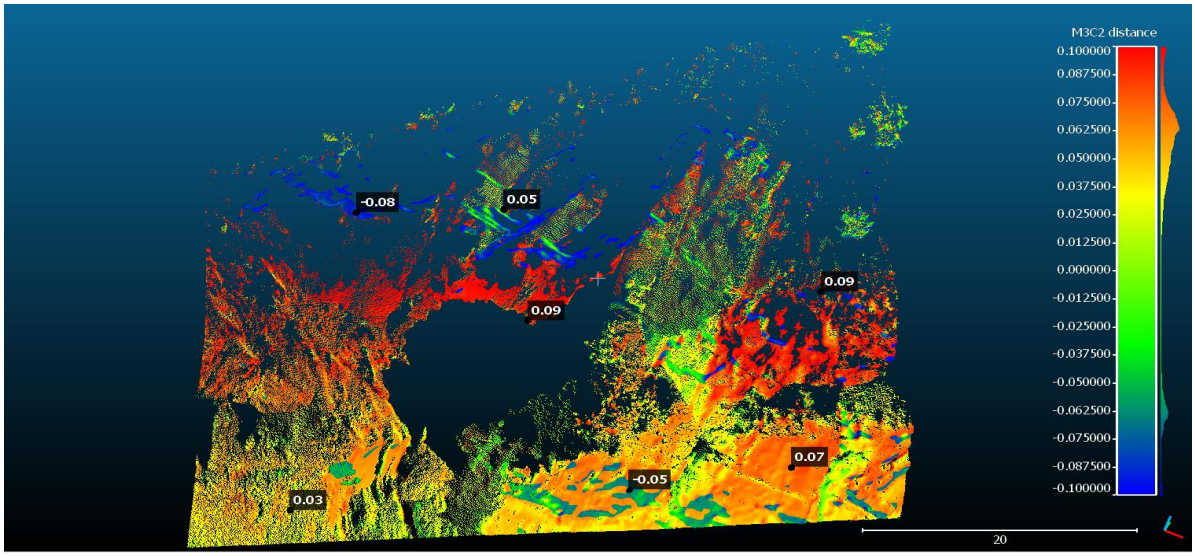

Figure 27. Displacement Heat Map of June - September Scans for Location 1 Along Z-Axis with a Scale of 10cm

4.2.1.2 Comparison of Displacement over Various Seasons

Similarly, M3C2 analyses were performed on June-September, September-December and December-April scans and results are shown in the Appendix. Table 13 presents the summary of the mean and standard deviation for all four pairwise displacement analyses for Location 1.

Table 13. Summary Statistics of M3C2 Analysis for Four Pairs of Scans for Location 1 (Unit: M)

Seasons	Mean (X-axis)	SD (X-axis)	Mean (Y-Axis)	SD (Y-Axis)	Mean (Z-Axis)	SD (Z-Axis)
June-September	0.055	0.030	-0.057	0.024	0.033	0.053
September-December	0.005	0.014	0.008	0.013	-0.007	0.013
December-April	-0.017	0.023	-0.025	0.012	0.021	0.019
June-April	-0.019	0.026	-0.026	0.020	0.021	0.025

From the Figure 28, it can be observed that major change in distance was observed between June and September scans. The least change was observed between September and December. Although

there was a change, the change was not significant. This is due to higher registration error and the relatively smaller mean distance change between scans.

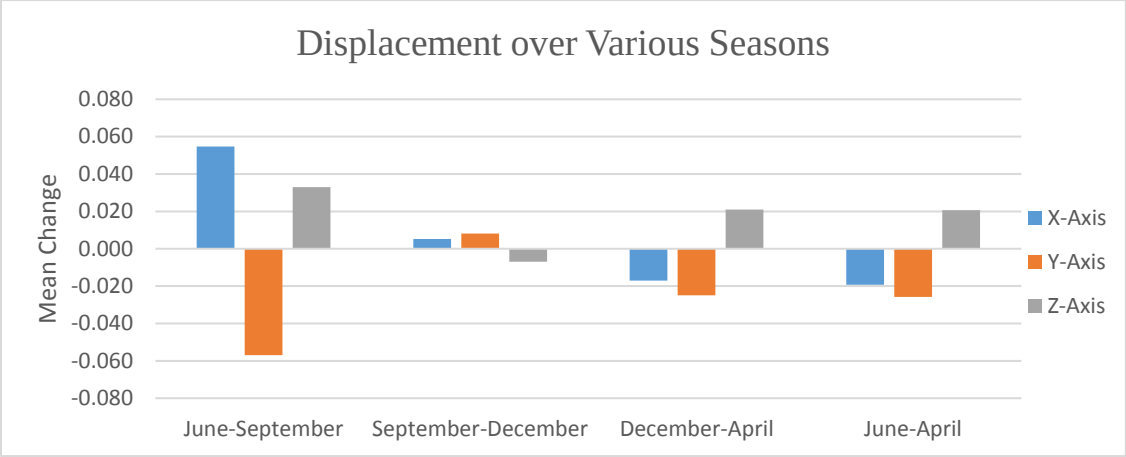

Figure 28. Displacement over Different Seasons

Figure 29 shows the heat map of the displacement in X Axis direction over various seasons for Location 1.

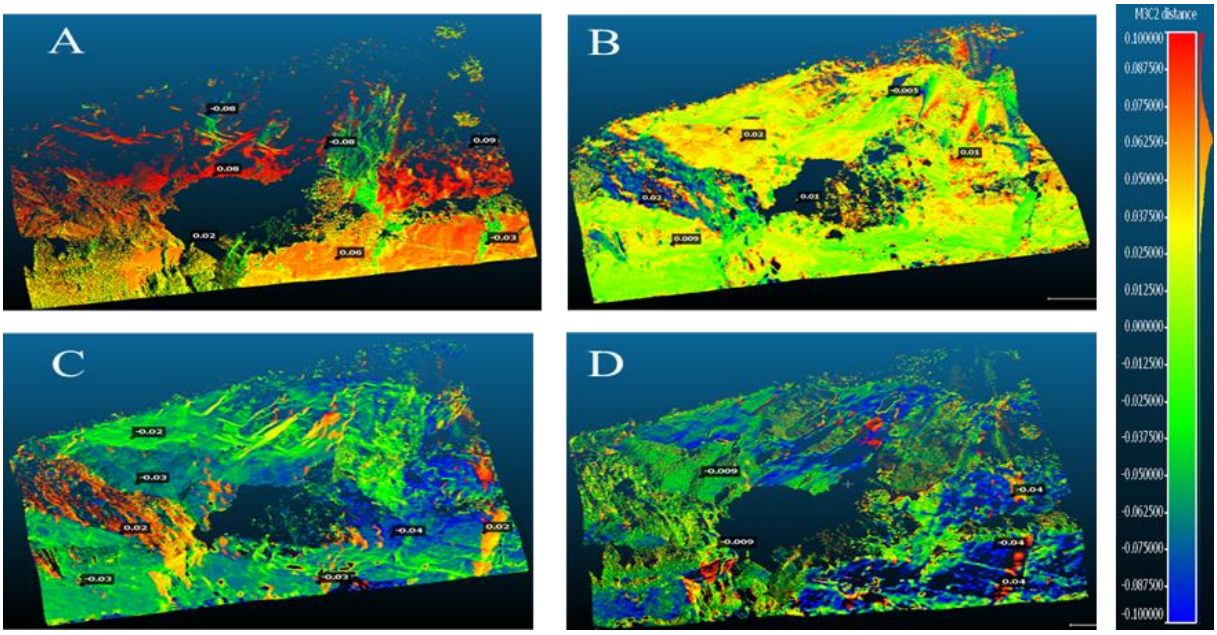

Figure 29. Displacement Heat Map for Location 1 along X-Axis for Various Seasons (Scale-10cm)

A. June-September B. September-December C. December-April D. June-April
Note: The values in each heat map represents the displacement (i.e. M3C2 distance) at that point.

4.3 M3C2 Analysis on Soil Type Location (Location 3)

Due to the presence of heavy vegetation and fewer planar surfaces, it was very difficult to register two different seasons' scans for Location 3. Compared to other seasons, better results were obtained for June and September scans with an error of 0.75. By considering this error, the M3C2 analysis was performed on June and September scans, and the results are shown below (Figure 30). From the results, it can be concluded that most of the displacement was not significant (Figure 30). This might be due to the presence of trees and a thick layer of grass on the surface. Several attempts were made to remove the vegetation, but the CANUPO algorithm didn't yield desirable results for Location 3 compared to Location 1. Because of the presence of a thick layer of grass, no land portion was able to be classified. Vegetation classification results of both Locations 1 and 3 are shown below (Figure 31), but the research team was not able to perform any meaningful analysis on other seasons' data because of large registration error.

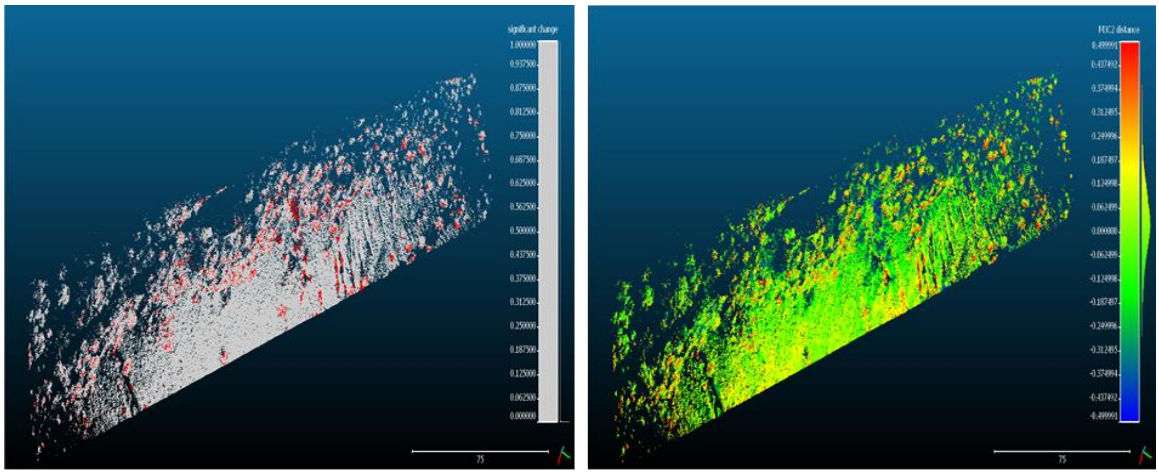

Figure 30. The Result of Significant Change Analysis (Left) and Displacement Heat Map (Right) for June and September Scans at Location 3

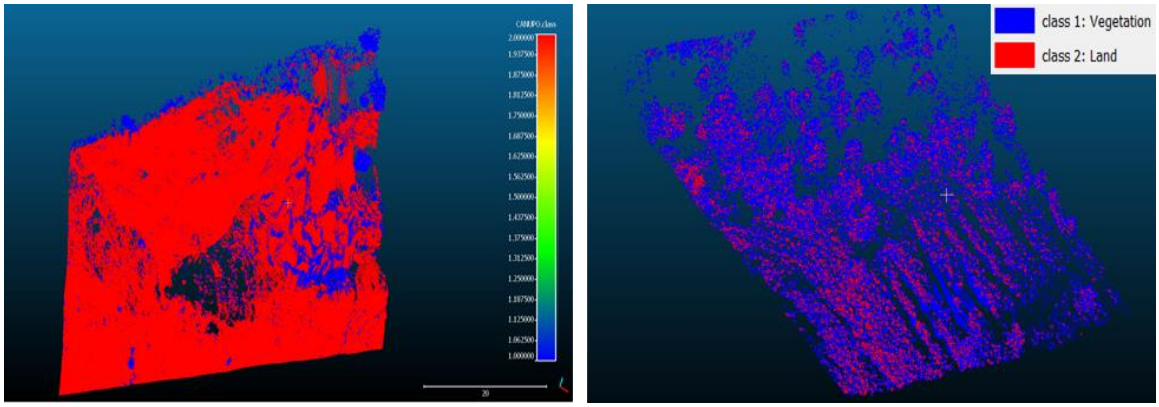

Figure 31. The Result of Vegetation and Land Classification for Location 1 (Left) and Location 3 (Right)

The above-shown heat map (Figure 30) is the result of M3C2 analysis with Normals oriented along X-Axis. A mean change of 0.028 meters with a standard deviation of 0.156 was observed along X-Axis. The significant change (red portion) shown in Figure 30 is due to the vegetation, so the change is not considered significant and results of the change in other orientations are not shown here due to the concern of space.

From Figure 31, it can be observed that the land portion and vegetation were perfectly classified for Location 1. Whereas for Location 3, even the vegetation was classified as land. The impacts of vegetation removal are discussed in the next section.

4.4 Impact of Vegetation Removal on M3C2 Analysis

In order to study the impact of vegetation removal on M3C2 analysis results, the vegetation removal was applied to Location 1. The results of original and vegetation removed data were compared. Figure 32 shows significant change analysis results and displacement heat maps (along X-axis) for the both original and vegetation removed data.

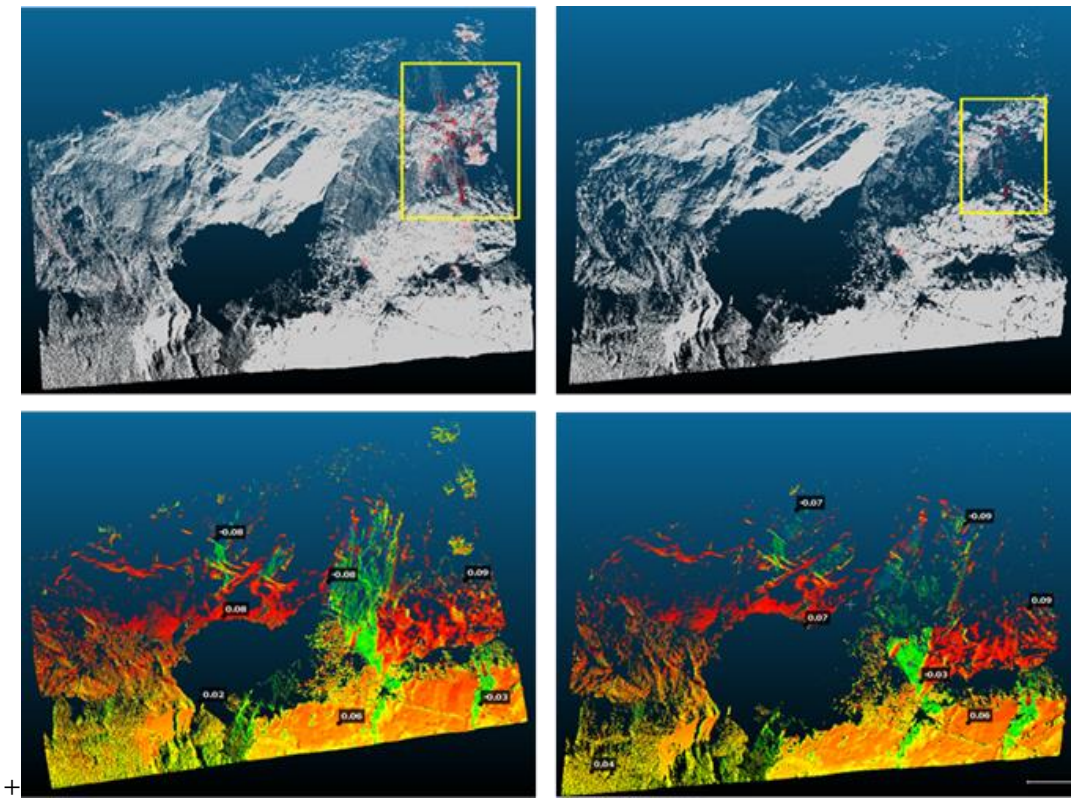

Figure 32. Significant Change Analysis Results (Top) and Displacement (Along X-axis) Heat Map (Bottom) of Original Patch (Left) and Vegetation Removed Patch (Right) at Location 1

From the above figure, it can be concluded that there is very little change in the displacement and the Gaussian statistics of the result are almost similar in the case of Location 1. However, there was slightly change observed in the significant change analysis. The significant change is represented in red; it can be observed that there is a smaller red portion in the vegetation removed patch compared to the original patch. The smaller red portion is due to the removal of change because of vegetation. In other words, the noise due to the vegetation in the significant change analysis was removed after vegetation removal. The significant change obtained in the case of vegetation removed data is a better representation of change. Whereas in the case of Location 3, if vegetation removal is achieved, there would be a considerable difference in both significant change analysis and displacement analysis results.

4.5 Impact of Downsampling on M3C2 Analysis

The impact of downsampling was studied on Location 1. The results of M3C2 on original and downsampled data are shown in Figure 33. The downsampling was performed on the data based on the spacing between the points using CloudCompare. The mean of the M3C2 distance of original data was 0.055 meters whereas for the downsampled data was 0.0183 meters. From this, it can conclude that downsampling affects statistical results of the analysis. Usually, downsampling is preferred when the data size is large. If downsampling is performed on smaller-sized data, the results would be similar to the one shown in Figure 33. The downsampled results on smaller size data, but the point cloud is often too sparse and hardly possible for visualization.

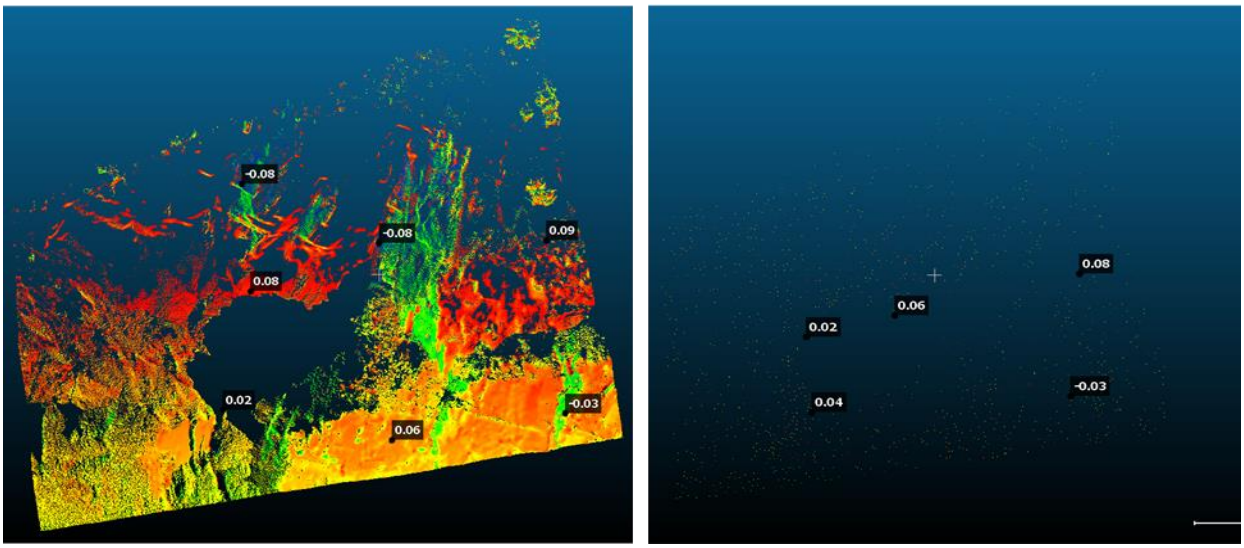

Figure 33. Displacement (Along X-axis) Heat Maps of Original (Left) and Downsampled (Right) Patch

4.6 Technical Challenges and Recommendations

Following are the major challenges experienced and lessons learned from the process of displacement analysis.

- The most important step before applying M3C2 analysis is registration of scans collected in two different seasons. The global registration error must be as minimum as possible to obtain accurate displacement results. Large portions of significant slope change were not able to be detected at 95% confidence level because of high registration errors in relation

to the magnitude of the actual slope displacement. The registration error was relatively higher for Locations 2 and 3 compared to Locations 1 and 2, due to the absence of planar surfaces and presence of thick vegetation at Locations 2 and 3. In order to overcome the registration challenge, suitable reflectors can be used to improve the registration.

- The M3C2 analysis was performed on Location 3 for June and September scans, but it was not possible with the data collected during other seasons because of poor registration results. Slightly better registration was possible in case of June and September scans because ICP algorithm was applied twice: one for the whole scene after coarse registration and the other one for a patch of the mountain considered for analysis. When tried to repeat the similar procedure for other seasons, the results were neither consistent nor desirable.
- The presence of a thick layer of grass resulted in poor M3C2 results for Location 3. In the case of rock type location, CANUPO algorithm worked very well since there was no layer of grass. Whereas in the case of soil slope (Location 3), the algorithm yielded only few ground points. Alternative algorithms need to be investigated, which is not the primary scope of this study.
- Mean change of the displacement analysis cannot be used as the only measure for slope over various seasons because the total registration error has an effect on the analysis. Therefore, both displacement heat maps and significant change analysis have to be jointly evaluated to get a clear picture of the slope change.

4.7 Generalized Workflow

Previous studies have used different workflows to apply terrestrial laser scanning technology to landslide monitoring. Basically, application of this technology needs to be customized, i.e., different tasks of processing are determined based on the characteristics of the site. Based on the above analysis, a more generalized workflow was developed for the application of laser scanning technology to measure the slope change for the sake of assessing the risk of landslides as shown in Figure 34. The most important step of the generalized workflow is preliminary site analysis; this is performed to obtain travel plan to locations, labor required, and a list of scanning and safety equipment. Apart from these, some of the features such as planar surfaces, reflecting objects of the site need to be analyzed, which may affect the decision on the registration algorithm used later to process the data. For this step, google maps, google earth, site specifications, and pictures can be

used. Moreover, personal trips to the sites need to be made. Another critical step of the generalized framework is visual check (VC). In visual check-1, the original patch should be verified before the process of registration, alignment, and vegetation. If there is thick vegetation and data is large in size, the data should go through a vegetation removal and downsampling process, respectively. After the data is processed with vegetation removal, the data needs to be visually checked (VC-2) to confirm whether vegetation is properly removed or not. In the case of downsampling, the data needs to be visually verified in terms of visibility. If VC-2 is passed, the processed data is subjected to M3C2 analysis. If VC-2 is failed, then the original point cloud patch has to be retreated with other algorithms, and the process is repeated until the data is satisfactory for further analysis.

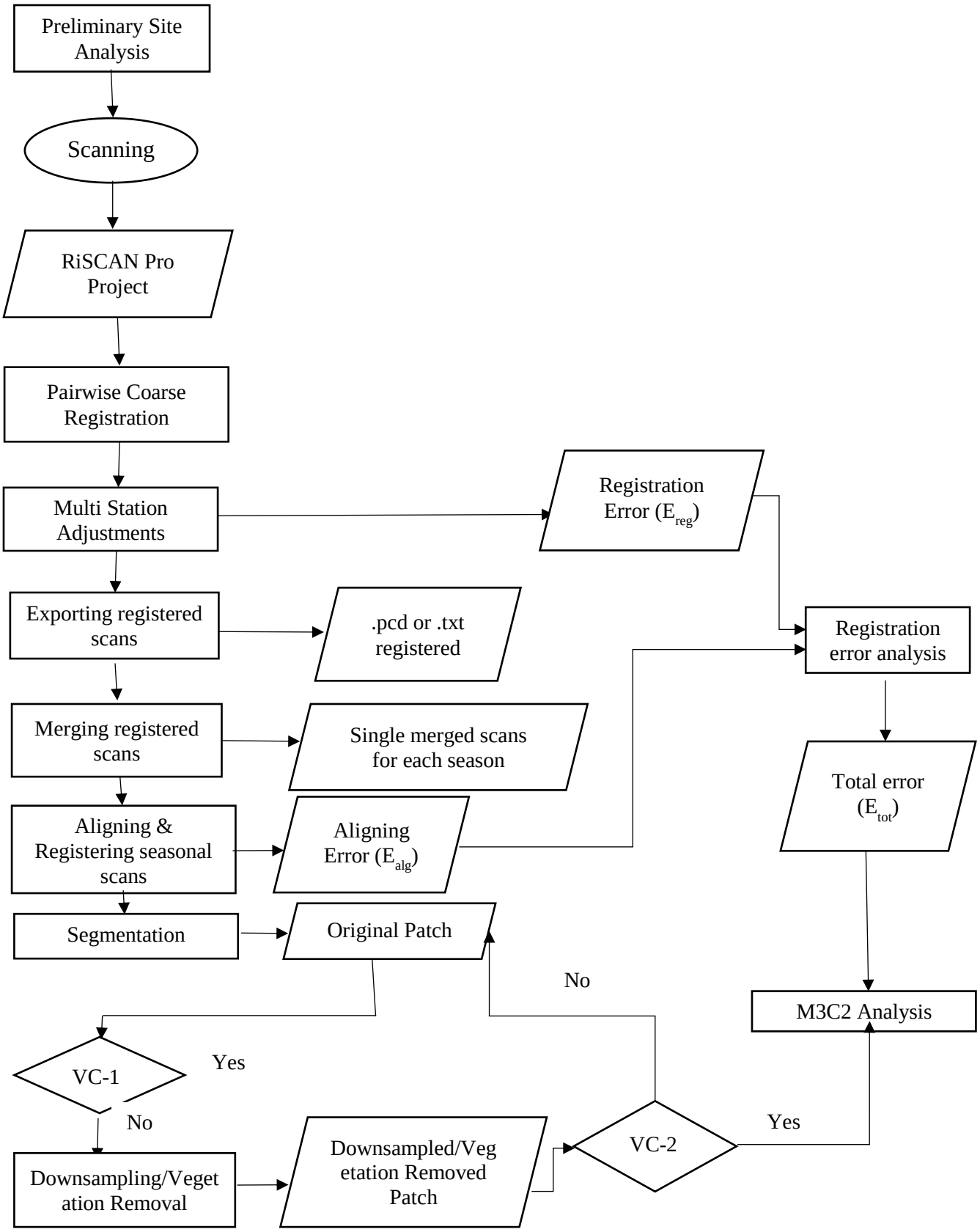

Figure 34. Generalized Workflow for Landslide Monitoring Using LiDAR

5. CONCLUSION

5.1 Main Findings and Recommendations

This study examined the use of terrestrial laser scanning to monitor the slope movement on the Oklahoma highways in the mountainous region. Through this study, a generalized workflow to apply terrestrial laser scanning technology for landslide monitoring on highways was developed, which can be applied to any site. During the process of developing a generalized framework, various data processing steps, such as registration and displacement analysis were evaluated. It can be concluded from the study that the registration algorithm has to be decided during the preliminary site analysis step based on the features (such as planar surfaces, reflecting objects) available on the site because early decisions will have a significant impact on the following processes. From the evaluation of various registration algorithms, it was observed that multi-station adjustment (MSA) with plane patch filter produced best results for Locations 0 and 1 since they have more planar surfaces. However, MSA did not work well with Locations 2 and 3 because of the presence of fewer planar surfaces and thick vegetation. Nevertheless, MSA still performed a better job on Locations 2 and 3 than ICP or NDT algorithms did. It was also observed from this study that it is not adequate to judge the goodness of the registration by solely relying on the statistics and that a visual check is very important at every stage of data processing. For example, in the case of ICP registration even though the RMS error is very small but the scans were completely misaligned. For Locations 2 and 3, registration of two different scans obtained in different seasons using ICP algorithm was difficult due to the presence of a thick layer of vegetation on the surface.

The M3C2 analysis provided a detailed understanding of the movement of the slopes. For Location 1, there was a higher displacement during June and September compared to other seasons. But it was observed that the change observed was not significant because of the relatively larger registration error. Whereas for soil type (Location 3) landslides, no meaningful displacement analyses were able to be performed primarily due to the noise of the grass and trees on the surface. Several attempts were made to filter vegetation, but very few ground points were obtained. Unfiltered data was used, and the displacement result was not significant, which is one of the limitations of this study.

The impact of vegetation removal on displacement analysis for Locations 0 and 1 proved that the results were improved after vegetation removal. The change observed due to the removal of the noise of vegetation, and more accurate results were obtained. Through this study, it is recommended that a visual check is required after the vegetation removal to make sure that land portion of the data is properly separated from vegetation. The study of downsampling's impact on the displacement analysis proved that the statistical results of displacement vary greatly due to downsampling. Therefore, it is recommended that downsampling should only be performed on large data.

Since the slope change on the majority of the portion of the slope was not statistically significant over the period of this research, a single year of monitoring is not sufficient to assess the risk of landslide/rockslide. These sites have to be continuously monitored for multiple years. In addition, the displacement analysis should be used in conjunction with geological characteristics of the site to better assess the risk of landslides/rockslides

This generalized framework and challenges reported by this study will help Oklahoma Department of Transportation (ODOT) apply laser scanning technology to monitor and assess the landslide risk on highways more effectively in the long run. Various challenges reported through this study not only helps in understanding the feasibility of this technology for monitoring landslides on highways but also directs researchers to address these issues.

The future work of this study should include the use of GPS unit for registration and compare the registration errors with the current process. There is a need for a robust algorithm for the registration of scans with no planar surfaces. Developing a tool using the proposed generalized workflow can help in the real-time processing of the data.

5.2 Landslide Mitigation Techniques

Monitoring the slope change is one of the effective approaches to observe the movement of the slopes and assess the risk of landslides. If the slope is believed to be in an unstable condition, proactive mitigation measures need to be taken to prevent the damage of landslides. Of course, there are a plethora of effective approaches to mitigating the impact of landslides on human life and property damages in the literature

.Landslide mitigation techniques include treatment of slope to prevent or control landslides (Fell 1994). The landslide mitigation techniques are mainly classified as structural and non-structural. Some of the structural techniques include slope stabilization, vegetation, drainage, channeling, groundwater improvement, and barriers such as walls, anchoring system, ramparts, and retaining structures. Non-structural techniques include land-use planning, emergency management, public awareness, etc. (Lacasse et al. 2009). Dai et al. (2002) have grouped various strategies to deal with landslides into engineering solution, planning control, acceptance, and warning system.

Choi and Cheung (2013) and Keaton and Eckhoff (1990) suggested a value engineering method that includes a risk-based framework. Value engineering approach tends to reduce the risk of the landslide to a satisfactory level while lowering the costs. Within an asset management framework, Li et al. (2009) and Loehr et al. (2004) recommended the use of decision analysis for cost effective geological hazards and related threats. The decision analysis used in asset management framework by Loehr et al. (2004) tends to balance the remedial costs associated with the uncertainty of their results. However, suitable frameworks have to be developed by individual transportation agencies in order to account for their system project protocol and cost structure.

WSDOT (2014) explained four basic strategies namely stabilization, protection, avoidance, and maintenance and monitoring. This report also compares reactive and proactive mitigation strategies. The reactive mitigation strategies impact the transportation facilities which also includes public reliability, convenience, and safety (Lowell 2013). Whereas, proactive strategies have some benefits over reactive mitigation methods, including cost effective, higher reliability, etc. However, it should be noted that proactive mitigation strategies do not necessarily dismiss the need for reactive methods because it is not possible to predict which slope fails first because when dealing with numerous unstable slopes.

Most of the landslide guidelines or reports reviewed in this study provide some guidance on the mitigation techniques. These guidelines view these topics at the different levels of details and provide approaches specific to the region. United States Transportation Board (Turner and Jayaprakash 1996) published a document titled “Landslide: Investigation and Mitigation”, explaining various approaches and techniques for investigation and mitigation for various types of landslides. The landslide management guideline (Caltrans 2003) issued by Department of Transportation of California explains various approaches to deal landslides and storm damage.

These guidelines provide various strategies for effective partnership and collaborative decision making among stake holders to enhance the process of landslide management on highways. The report provides an overview of geological characteristics and landslides along the California's Big Sur Coast highway corridor as well as programs for landslide management activities, integrated approach for decision making, and best landslide mitigation techniques. Even though the guidelines are specific to Big Sur corridor, these strategies can be applied to other locations with suitable changes. Choi and Cheung (2013) have presented the evolution of Landslip Prevention Programme (LPM) and Landslip Prevention and Mitigation (LPMit) Programme implemented by Hong Kong government. This case study is an excellent example of developing an integrated landslide mitigation system

.

REFERENCES

Abdel-Razek, R. H. (1997). "How construction managers would like their performance to be evaluated." *Journal of construction engineering and management*, 123(3), 208-213.

Aguilar, F. J., Mills, J. P., Delgado, J., Aguilar, M. A., Negreiros, J., and Pérez, J. L. (2010). "Modelling vertical error in LiDAR-derived digital elevation models." *ISPRS Journal of Photogrammetry and Remote Sensing*, 65(1), 103-110.

Al-Durgham, K., Habib, A., and Kwak, E. "RANSAC approach for automated registration of terrestrial laser scans using linear features." *Proc., ISPRS Annals of Photogrammetry, Remote Sensing and Spatial Information Sciences: ISPRS Workshop Laser Scanning 2013*, 11-13.

Cerator, A.B., Hong, Yang, and Tabe, W. (2014). "Ral Time Monitoring of Slope Stability in Eastern Oklahoma."Oklahoma Department of Transportation

Bae, K.-H., and Lichti, D. D. (2008). "A method for automated registration of unorganised point clouds." *ISPRS Journal of Photogrammetry and Remote Sensing*, 63(1), 36-54.

Baldo, M., Bicocchi, C., Chiocchini, U., Giordan, D., and Lollino, G. (2009). "LIDAR monitoring of mass wasting processes: The Radicofani landslide, Province of Siena, Central Italy." *Geomorphology*, 105(3), 193-201.

Bates, R. L., and Jackson, J. A. "1987." *Glossary of geology (third edition): Alexandria, Virginia, American Geological Institute*.

Becerik-Gerber, B., Jazizadeh, F., Kavulya, G., and Calis, G. (2011). "Assessment of target types and layouts in 3D laser scanning for registration accuracy." *Automation in Construction*, 20(5), 649-658.

Beinat, A., Crosilla, F., and Sepic, F. (2006). "Automatic morphological pre-alignment and global hybrid registration of close range images." *International Archives of the Photogrammetry, Remote Sensing and Spatial Information Sciences*, 36(part 5), 25-27.

Beinat, A., Crosilla, F., Visintini, D., and Sepic, F. (2007). "Automatic non parametric procedures for terrestrial laser point clouds processing." *International Archives of Photogrammetry, Remote Sensing and Spatial Information Sciences*, 36(3), W49B.

Besl, P. J., and McKay, N. D. "Method for registration of 3-D shapes." *Proc., Robotics-DL tentative*, International Society for Optics and Photonics, 586-606.

Boström, G., Gonçalves, J. G., and Sequeira, V. (2008). "Controlled 3D data fusion using error-bounds." *ISPRS Journal of Photogrammetry and Remote Sensing*, 63(1), 55-67.

Brodu, N., and Lague, D. (2012). "3D terrestrial lidar data classification of complex natural scenes using a multi-scale dimensionality criterion: Applications in geomorphology." *ISPRS Journal of Photogrammetry and Remote Sensing*, 68, 121-134.

Caltrans (2003). "Guidelines for Landslide Management and Storm Damage Response."

Canaz, S. (2012). "Planar and linear feature-based registration of terrestrial laser scans with minimum overlap using photogrammetric data." Doctoral Dissertation, University of Calgary.

Casson, B., Delacourt, C., and Allemand, P. (2005). "Contribution of multi-temporal remote sensing images to characterize landslide slip surface? Application to the La Clapière landslide (France)." *Natural Hazards and Earth System Science*, 5(3), 425-437.

Chan, T. O., Lichti, D. D., and Glennie, C. L. (2013). "Multi-feature based boresight self-calibration of a terrestrial mobile mapping system." *ISPRS journal of photogrammetry and remote sensing*, 82, 112-124.

Chang, Y.-C., Detchev, I., and Habib, A. "A Photogrammetric system for 3D reconstruction of a scoliotic torso." *Proc., Proceedings of the ASPRS 2009 Annual Conference*.

Chen, S.-E., Liu, W., Bian, H., and Smith, B. (2013). "3D LiDAR scans for bridge damage evaluations." *Forensic Engineering 2012: Gateway to a Safer Tomorrow*, 487-495.

Choi, K. Y., and Cheung, R. W. M. (2013). "Landslide disaster prevention and mitigation through works in Hong Kong." *Journal of Rock Mechanics and Geotechnical Engineering*, 5(5), 354-365.

Collins, B. D., Minasian, D. L., and Kayen, R. (2009). "Topographic change detection at select archeological sites in Grand Canyon National Park, Arizona, 2006-2007." US Geological Survey.

Conner, J. C. (2013). "Quantification of landslide movement in a forested environment."

Conner, J. C., and Olsen, M. J. (2014). "Automated quantification of distributed landslide movement using circular tree trunks extracted from terrestrial laser scan data." *Computers & Geosciences*, 67, 31-39.

Daehne, A., and Corsini, A. (2013). "Kinematics of active earthflows revealed by digital image correlation and DEM subtraction techniques applied to multi- temporal LiDAR data." *Earth Surface Processes and Landforms*, 38(6), 640-654.

Dai, F. C., Lee, C. F., and Ngai, Y. Y. (2002). "Landslide risk assessment and management: an overview." *Engineering Geology*, 64(1), 65-87.

Dewitte, O., Jasselette, J.-C., Cornet, Y., Van Den Eeckhaut, M., Collignon, A., Poesen, J., and Demoulin, A. (2008). "Tracking landslide displacements by multi-temporal DTMs: A combined aerial stereophotogrammetric and LIDAR approach in western Belgium." *Engineering Geology*, 99(1), 11-22.

Dold, C., and Brenner, C. (2006). "Registration of terrestrial laser scanning data using planar patches and image data." *International Archives of Photogrammetry, Remote Sensing and Spatial Information Sciences*, 36(5), 78-83.

Fell, R. (1994). "Landslide risk assessment and acceptable risk." *Canadian Geotechnical Journal*, 31(2), 261-272.

FEMA, (Federal Emergency Management Agency 2017). "Causes and Types of Landslides." <http://www.fema.gov/media-library-data/20130726-1440-20490-6324/fema_182_chapter3_part1.pdf.>. (June 10, 2017).

Fernandez Merodo, J. A., Pastor, M., Mira, P., Tonni, L., Herreros, M. I., Gonzalez, E., and Tamagnini, R. (2004). "Modelling of diffuse failure mechanisms of catastrophic landslides." *Computer Methods in Applied Mechanics and Engineering*, 193(27-29), 2911-2939.

Habib, A., Kersting, A. P., Bang, K. I., and Lee, D.-C. (2010). "Alternative methodologies for the internal quality control of parallel LiDAR strips." *IEEE Transactions on Geoscience and Remote Sensing*, 48(1), 221-236.

Habib, A., Kwak, E., and Al-Durgham, M. (2011). "Model-based automatic 3d building model generation by integrating lidar and aerial images." *Archiwum Fotogrametrii, Kartografii i Teledetekcji*, 22.

Haugen, B. D. (2016). *Qualitative and quantitative comparative analyses of 3D lidar landslide displacement field measurements*. Masters Thesis, Colorado School of Mines.

Hodgson, M. E., and Bresnahan, P. (2004). "Accuracy of airborne lidar-derived elevation." *Photogrammetric Engineering & Remote Sensing*, 70(3), 331-339.

Hofton, M. A., Minster, J. B., and Blair, J. B. (2000). "Decomposition of laser altimeter

waveforms." *IEEE Transactions on geoscience and remote sensing*, 38(4), 1989-1996.
Huang, T., Zhang, D., Li, G., and Jiang, M. (2012). "Registration method for terrestrial LiDAR point clouds using geometric features." *Optical Engineering*, 51(2), 021114-021111-021114-021115.
Jaselskis, E. J., Gao, Z., and Walters, R. C. (2005). "Improving transportation projects using laser scanning." *Journal of Construction Engineering and Management*, 131(3), 377-384.
Keaton, J. R., and Eckhoff, D. W. (1990). "Value engineering approach to geologic hazard risk management." *Transportation Research Record*(1288).
Kinzel, P. J., Wright, C. W., Nelson, J. M., and Burman, A. R. (2007). "Evaluation of an experimental LiDAR for surveying a shallow, braided, sand-bedded river." *Journal of Hydraulic Engineering*, 133(7), 838-842.
Lacasse, S., Nadim, F., Lacasse, S., and Nadim, F. (2009). "Landslide Risk Assessment and Mitigation Strategy." *Landslides – Disaster Risk Reduction*, K. Sassa, and P. Canuti, eds., Springer Berlin Heidelberg, Berlin, Heidelberg, 31-61.
Lague, D., Brodu, N., and Leroux, J. (2013). "Accurate 3D comparison of complex topography with terrestrial laser scanner: Application to the Rangitikei canyon (NZ)." *ISPRS Journal of Photogrammetry and Remote Sensing*, 82, 10-26.
Li, Z., Huang, H., Xue, Y., and Yin, J. (2009). "Risk assessment of rockfall hazards on highways." *Georisk*, 3(3), 147-154.
Libraries, P. C. "VoxelGrid Filter." <http://pointclouds.org/>. (05/18/2017).
Loehr, J. E., Bernhardt, K. S., and Huaco, D. R. (2004). "Decision support for slope construction and repair activities: an asset management building block."
Lowell, S. M. a. N. I. N. (2013). *Chapter 18: Rockfall management programs, in Rockfall: Characterization and Control*, A.K. Turner and R.L. Schuster, Transportation Research Board.
Mapping, D. L. (2013). "RiSCAN PRO Data Registration Guide." <https://s3-eu-west-1.amazonaws.com/3dlmsitecontent/police/documents/RiSCAN_PRO_DataRegistrationGuide_v2_low-res.pdf>. (06/12/2017).
NewsOn6 (June 22 2015). "Rockslide Continues To Hold Up Traffic Near Davis." <http://www.newson6.com/story/29380996/rockslide-continues-to-hold-up-traffic-near-davis>.
OGS (Oklahoma Geological Survey 2017). "OGS Earthquake Information." <https://earthquakes.ok.gov/>. (Feburary 21 2017).
Pfeiffer, T. J., Higgins, J. D., Andrew, R. D., Barrett, R. K., and Beck, R. B. (1993). *Colorado Rockfall Simulation Program: Version 3.0 User's Manual*, Colorado Department of Trans.
Priestnall, G., Jaafar, J., and Duncan, A. (2000). "Extracting urban features from LiDAR digital surface models." *Computers, Environment and Urban Systems*, 24(2), 65-78.
Rabbani, T., Dijkman, S., van den Heuvel, F., and Vosselman, G. (2007). "An integrated approach for modelling and global registration of point clouds." *ISPRS journal of Photogrammetry and Remote Sensing*, 61(6), 355-370.
Renslow, M. S. (2012). *Manual of airborne topographic lidar*.
Reshetyuk, Y. (2010). "Direct georeferencing with GPS in terrestrial laser scanning." *Z f V-Zeitschrift für Geodäsie, Geoinformation und Landmanagement*, 135(3), 151-159.
Rodrigues, M., Fisher, R., and Liu, Y. (2002). "Special Issue on registration and fusion of range images." *Computer Vision and Image Understanding*, 87(1-3), 1-7.
Rosen, P. A., Hensley, S., Joughin, I. R., Li, F. K., Madsen, S. N., Rodriguez, E., and Goldstein,

R. M. (2000). "Synthetic aperture radar interferometry." *Proceedings of the IEEE*, 88(3), 333-382.

Rusinkiewicz, S., and Levoy, M. "Efficient variants of the ICP algorithm." *Proc., 3-D Digital Imaging and Modeling, 2001. Proceedings. Third International Conference on*, IEEE, 145-152.

S. Falemo, and Andersson-Sköld, Y. (2011). "Landslide consequence analysis – mapping expected losses in the Göta river valley." *ISGSR*, Bundesanstalt für Wasserbau.

Schneider, D., and Maas, H.-G. "Integrated bundle adjustment with variance component estimation-fusion of terrestrial laser scanner data, panoramic and central perspective image data." *Proc., Proceedings ISPRS Workshop Laser Scanning, and SilviLaser*, Citeseer, 373.

Shao-tang Liu, and Wang, Z.-w. (2008). "Choice of surveying methods for landslides monitoring."

USGS (United State Geological Survey 2004). "Fact sheet 2004-03072: Landslide Types and Processes." <https://pubs.usgs.gov/fs/2004/3072/fs-2004-3072.html>. (February 22, 2017)

Turner, A. K., and Jayaprakash, G. (1996). *LANDSLIDES: INVESTIGATION AND MITIGATION. CHAPTER 1-INTRODUCTION*.

USGS (2017). "Landslide Hazards Program." <http://landslides.usgs.gov/monitoring/>. (February 22, 2017).

Varnes, D. J. (1984). *Landslide hazard zonation: a review of principles and practice.*

Vosselman, G., and Maas, H.-G. (2010). *Airborne and terrestrial laser scanning*, Whittles Publishing.

Vosselman, G., and Maas, H. (2010). "Airborne and terrestrial laser scanning." CRC Press, Boca Raton.

Wang, G. (2011). "GPS landslide monitoring: single base vs. network solutions—a case study based on the Puerto Rico and the Virgin Islands permanent GPS network." *Journal of Geodetic Science*, 1(3), 191-203.

Wehr, A., and Lohr, U. (1999). "Airborne laser scanning—an introduction and overview." *ISPRS Journal of Photogrammetry and remote sensing*, 54(2), 68-82.

Whittow, J. B. (1984). "The Penguin dictionary of physical geography." Penguin Books Harmondsworth.

Wieczorek, G. F., and Snyder, J. B. (2009). "Monitoring slope movements." *Geol. Monit*, 245-271.

Wold, R. L., and Jochim, C. L. (1989). "Landslide loss reduction: A guide for state and local government planning." *Earthquake Hazards Reduction Series*, US Federal Emergency Management Agency (FEMA).

WSDOT (Washington Department of Transportation 2014). "Landslide Mitigation Action Plan.", WSDOT, Olympia, WA.

APPENDIX

Coarse and Fine Registration Using RiSCAN Pro

The link below explains coarse registration and Multi-Station Adjustments using RiSCAN on Location 1 data.

Link for Coarse and Fine Registration using RiSCAN Pro :

(https://drive.google.com/open?id=0B0W26tsi2OuVT1IyZTZSZDBCMEk)

M3C2 Analysis of September and December Scans for Location 1

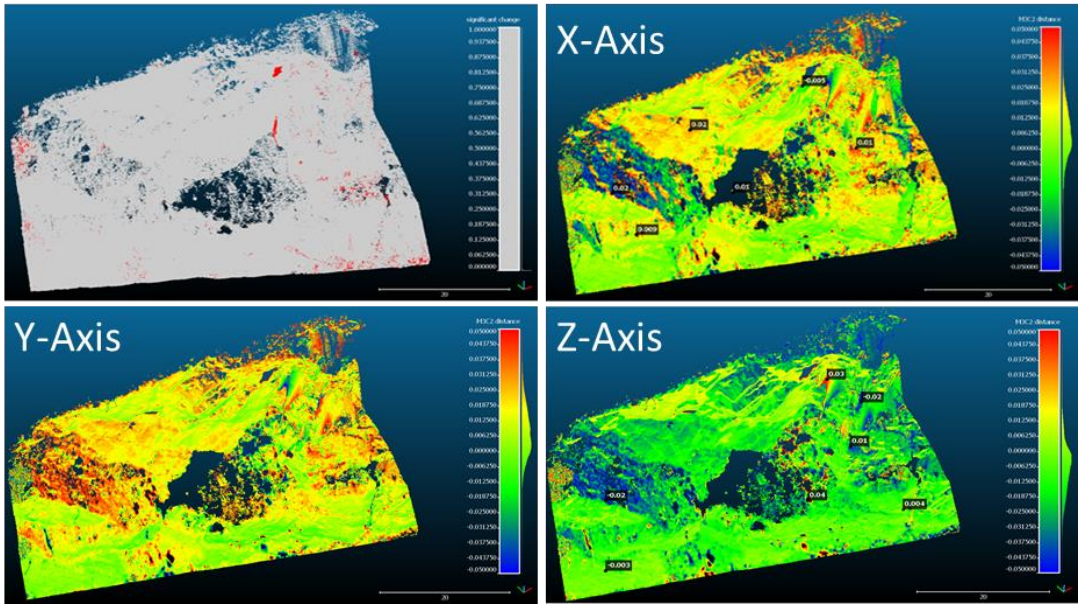

Figure A- 1. Significant Change and Displacement Heat Map of September and December Scans for Location 1 along X, Y and Z Axes (Scale 5cm)

M3C2 Analysis of December and April Scans for Location 1

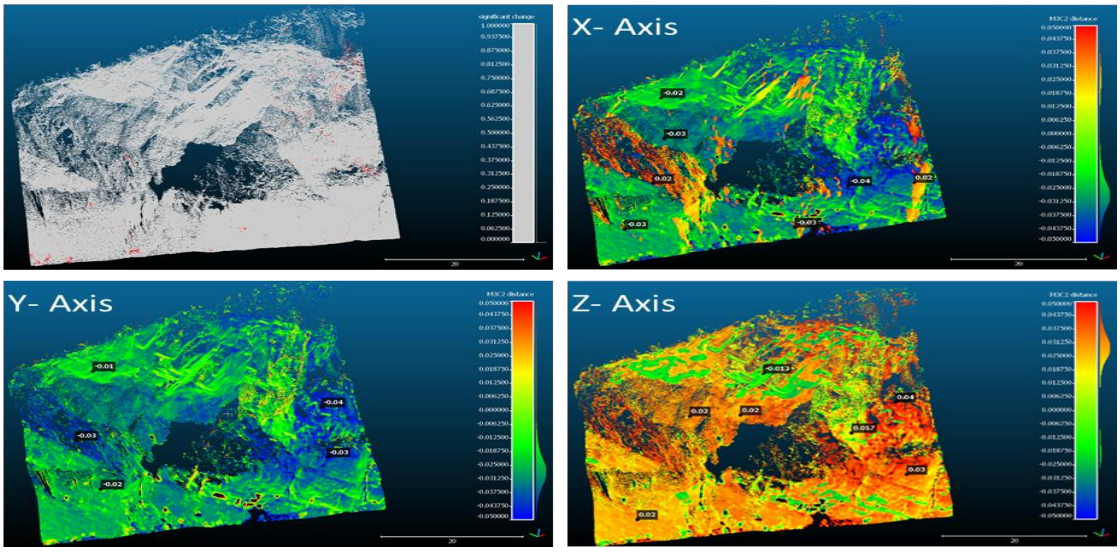

Figure A- 2. Significant Change and Displacement Heat Map of December and April Scans for Location 1 along X, Y and Z Axes (Scale 5cm)

M3C2 Analysis of December and April Scans for Location 1

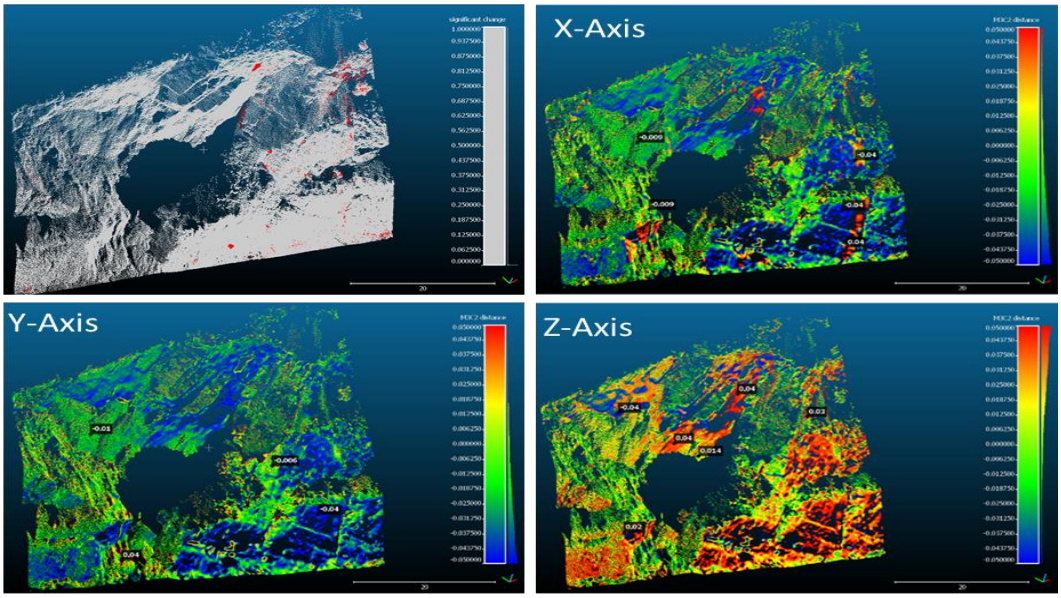

Figure A- 3. Significant Change and Displacement Heat Map of June and April Scans for Location 1 along X, Y and Z Axes (Scale 5cm)